DOT/FAA/AM- 25/19

Office of Aerospace Medicine

Washington, D.C. 20591

Occupant Response to Varying Seat Stroke Using a Reusable Energy Attenuating Aircraft Seat

Ian T. Hellstrom

David M. Moorcroft

William H. Carroll

Civil Aerospace Medical Institute (CAMI)

Federal Aviation Administration

Oklahoma City, OK 73169

December 2025

NOTICE

This document is disseminated under the sponsorship of the U.S. Department of Transportation in the interest of information exchange. The United States Government assumes no liability for the contents thereof.

This publication and all Office of Aerospace Medicine technical reports are available in full text from the Civil Aerospace Medical Institute's publications website and at the National Transportation Library's Repository & Open Science Access Portal.

Technical Report Documentation

1. Report No. DOT/FAA/AM-25/19	2. **Report Date** December 2025
3. **Title & Subtitle** Occupant Response to Varying Seat Stroke Using a Reusable Energy Attenuating Aircraft Seat	**4. Performing Organization Code** AAM-632
5. Author(s) Hellstrom, Ian T. (ORCID 0000-0002-3972-3981) Moorcroft, David M. (ORCID 0000-0002-9709-1150) Carroll, William H. (ORCID 0000-0001-6668-6971)	**6. Performing Org Report Number** DOT/FAA/AM-25/19
7. Performing Organization Name & Address Civil Aerospace Medical Institute Federal Aviation Administration Oklahoma City, OK 73169	8. **Contract or Grant Number** None
9. Sponsoring Agency Name & Address Aircraft Certification Service (AIR) Federal Aviation Administration 800 Independence Ave., S.W. Washington, DC 20591	**10. Type of Report & Period** Technical Report

11. Supplementary Notes

Project Sponsor: Joseph Pellettiere. Technical report DOI: https://doi.org/10.21949/1529692

The Federal Aviation Administration (FAA) funded this through the Research, Engineering, and Development (RE&D) program budget. The authors had no conflicts of interest to disclose. All authors read and approved this manuscript. This manuscript underwent an external peer review. The authors collected the data, performed the data analysis, and wrote the technical report. This document is disseminated under the sponsorship of the U.S. Department of Transportation in the interest of information exchange. The U.S. Government assumes no liability for the contents thereof.

12. Abstract

While the U.S. rotorcraft accident rate over the past 10 years has steadily decreased, the number of fatal rotorcraft accidents and fatalities remains virtually unchanged. Survival in many impact scenarios is directly related to the certification level of the rotorcraft. Seats installed in newly designed rotorcraft must meet the emergency landing dynamic conditions rule (14 CFR Part 27.562 and §29.562). Rotorcraft with existing type certificates, whether newly manufactured or not, do not need to meet the dynamic rule. Many legacy rotorcraft have limited space beneath the existing seats, this precludes the use of a retrofitted fully compliant stroking seat. However, these rotorcraft could still benefit from meeting the framework of the rule with a reduced velocity requirement. The FAA Civil Aerospace Medical Institute conducted research on the relationship between impact pulse, seat stroke, and occupant injury risk. 48 tests were run using a rigid Reusable Energy Attenuating Laboratory (REAL) Seat, designed by the Navy, that allowed for varying seat stroke between tests. Results showed a strong correlation between seat stroke distance and lumbar load (R^2>0.97), as well as pelvis acceleration and lumbar load. Comparing the data from this test series to 88 tests from the CAMI database showed that the relationship between pelvic acceleration and lumbar load is dependent on the sled acceleration. These findings may support updates to advisory circulars and guide future rulemaking to enhance rotorcraft crashworthiness.

13. Key Word Anthropomorphic Test Device, ATD, Certification Testing, Pelvis Acceleration, Lumbar-Spine Load, Seat-Pan Acceleration, Floor Load, Photometrics, Aircraft Seats, Acceleration		**14. Distribution Statement** Document is available to the public through: National Transportation Library: https://ntl.bts.gov/ntl
15. Security Classification (of this report) Unclassified	**16. Security Classification (of this page)** Unclassified	**17. No. of Pages** 42

Author Note

Funding	The research was accomplished using FAA RE&D funding programmed through the aeromedical research budget (project # A11J.RS1).
Conflicts of Interest	The authors had no conflicts of interest to disclose.
Author Contributions	Hellstrom: (Data Collection, Data Analysis, & Report Writing) Moorcroft: (Data Collection, Data Analysis, & Report Writing), Carroll: (Data Collection, Data Analysis & Report Writing)
Data Availability	Technical report DOI: https://doi.org/10.21949/1529692, Data available at: https://doi.org/10.21949/1529693.

Acknowledgments

Research reported in this paper was sponsored by the FAA Office of Aircraft Certification Service and conducted by the Aerospace Medical Research Division, Protection and Survival Research Branch, Engineering Sciences Section, Biodynamics Research Team (AAM-632) at the FAA Civil Aerospace Medical Institute (CAMI). The work was carried out under RE&D control account number A11J.RS.1 and could not have been completed without the full support of the technical staff at CAMI: Jeff Ashmore, Ronnie Minnick, and Zachary Perkins. We also thank Hilary Uyhelji for subject matter expertise that informed the appendix, and personnel from the United States Navy (Naval Air Station Patuxent River) for information sharing that enabled development of a Reusable Energy Attenuating Laboratory (REAL) Seat for the FAA CAMI facility. We appreciate the peer review comments provided by Lindley Bark (United States Navy), Martin Crane (Federal Aviation Administration), and Amanda Taylor (Federal Aviation Administration). Additional thanks to Amanda Taylor for initiating the project, providing project management, and contributing to the testing protocol prior to transferring project responsibilities.

Table of Contents

List of Figures

List of Tables

List of Abbreviations

ARAC	Aviation Rulemaking Advisory Committee
ATD	anthropometric test device
CG	center of gravity
CAMI	Civil Aerospace Medical Institute
CF	Confor™ Foam
CFR	Code of Federal Regulations
CMM	coordinate measuring machine
CSDG	Crash Survival Design Guide
DRI	dynamic response index
FAA	Federal Aviation Administration
ft/sec	feet per second
g	gravity
H-point	hip point
in.	inch
in.-lb.	inch-pounds force
JSSG	Joint Service Specification Guide
lb.	pounds force
ms	milliseconds
NASA	National Aeronautics and Space Administration
N_{ij}	neck injury criteria
psi	pounds per square inch
REAL Seat	reusable energy attenuating laboratory seat
ROPWG	Rotorcraft Occupant Protection Working Group
THOR	Test device for Human Occupant Restraint

Background

While the U.S. rotorcraft accident rate in recent years has steadily decreased, the number of fatal rotorcraft accidents and fatalities remains virtually unchanged (Federal Register, 2015). Blunt-force trauma was the cause of death in 92% of fatalities studied from 2008-2013 (Roskop, 2017). A more recent survey of the National Transportation Safety Board accident data covering 2009-2018 shows similar trends (Taylor, Pellettiere, 2022). Survival in many impact scenarios is directly related to the safety certification level of the rotorcraft. Rotorcraft seats are required to meet the Emergency Landing Dynamic Conditions Rule (hereafter, the "dynamic rule"), 14 CFR §27.562 (and §29.562 for transport-category rotorcraft) for all newly designed rotorcraft.

There are two test conditions defined by the dynamic rule. One is a vertical-impact condition with a minimum impact velocity of 30 ft/sec, peak acceleration of 30 g, and an impact angle of 30° off vertical. In this test, the principal measurement is the compressive load in the lumbar spinal column, which has a regulatory limit of 1500 lb.

Although the rotorcraft dynamic rule had an effective date of December 1989, by 2017 only approximately 10% of the U.S. civilian rotorcraft fleet was compliant, as there was no retrofit requirement for rotorcraft with existing type certificates (Roskop, 2017; Federal Register, 2015). An analysis of 184 accidents that occurred between 2009 and 2018 showed that only 12 (6.5%) were fully compliant for crash resistant seats and structures (Taylor, Pellettiere 2022). On November 5, 2015, the Federal Aviation Administration (FAA) tasked the Aviation Rulemaking Advisory Committee (ARAC) to provide recommendations regarding occupant protection rulemaking in normal- and transport-category rotorcraft for older certification-basis type designs that are still in production (referred to as "legacy rotorcraft").

The ARAC formed the Rotorcraft Occupant Protection Working Group (ROPWG) to study and provide recommendations on these issues. Because many rotorcraft have long operational lives, ARAC considered fleet attrition (i.e. replacement of older models with new models meeting §27/29.562) too slow to achieve a timely reduction in fatal accidents, and therefore unacceptable (Federal Register, 2015).

ARAC Recommendations

The ARAC published two reports: a cost benefit analysis in 2016 and a set of recommendations for crashworthiness in 2018 (ROPWG, 2016; ROPWG, 2018). The 2018 report contains recommendations for incorporating the requirements of all or part of 14 CFR 27/29.561, §27/29.562, and §27/29.785 into rotorcraft with approved type certificates before these regulations went into effect. The ROPWG noted that blunt force injuries are a significant source of injuries in civil helicopter crashes. However, they also noted that incorporating the existing regulations into current rotorcraft designs is impeded by several technical and economic issues.

Regarding dynamic seat testing in the vertical direction as specified in §27.562(b)(1), the report recommended adopting the Part 27 regulation with changes:

Reduction in spinal injuries is a high priority for occupant protection, but some legacy Part 27 models have insufficient space under certain seats to meet the full requirement. Requiring them to retrofit with fully compliant seats would lead to the discontinuation of these models. However, seats rated to a 21.7 ft/sec vertical impact could be incorporated into nearly all seats in existing helicopters and would provide 71% of the protection afforded by fully compliant seats. The

ROPWG therefore recommended full compliance in those seat places where practicable, and a reduced velocity of 25 ft/sec (21.7 ft/sec vertical component) in only those seating positions where full compliance is impracticable (ROPWG, 2018). Reduction from the existing 2X.562 test requirements is only being evaluated for retrofit and new manufacturing of old type designs. The FAA does not intend to modify the requirements for new rotorcraft designs.

For Part 29 rotorcraft, the report recommended adopting §29.562(b)(1) in existing type designs without change. These rotorcraft are larger than their Part 27 counterparts, the ARAC noted, "the cost and weight penalties associated with full compliance are relatively small for Part 29 helicopters. There is no known significant impediment to requiring the full regulation for Part 29 helicopters other than a possible small reduction in seating capacity in some models."

The 2016 ARAC report noted that meeting the requirement for vertical energy absorption of the seat requires a minimum stroking distance and this distance was not practicably available in existing small and medium sized rotorcraft (ROPWG, 2016). This is due to some seating positions being mounted on top of fuel tanks or control system components. The minimum stroking distance was based, at least in part, from the Analysis of Rotorcraft Crash Dynamics for Development of Improved Crashworthiness Design Criteria[1], which reported that to meet the recommended energy absorber load limit of 12 g, the required stroke distance would be 3.8 – 4.5 inches (in.) (50^{th} - 95^{th} percentile male occupants) (Coltman, et. al., 1985, Pg 87). The ARAC separately calculated that 4.6 in. of stroke would be necessary to meet the 1500 lb. lumbar load criterion for the 30 ft/sec pulse (26 ft/sec vertical component), while 2.8 in. is necessary for the 25 ft/sec pulse (Rotorcraft Occupant Protection Working Group, 2018). It was also noted that the 26 ft/sec vertical impact velocity specified in §27/29.562(b)(1) corresponds to the 95^{th} percentile vertical impact velocity occurring in survivable accidents (Coltman, et.al. 1985). The 90^{th} percentile accident corresponds to a 21.7 ft/sec vertical impact velocity.

Their key takeaway is that:

> Since a 21.7 ft/sec vertical dynamic seat test would provide most of the protection of a 26 ft/sec seat, but with much less disruption to the industry, the ROPWG believes that for seating positions in Part 27 helicopters ,where it is not practicable to accommodate 26 ft/sec vertical velocity requirement seats, a 21.7 ft/sec vertical velocity requirement seat provides a reasonable compromise for increasing occupant protection, in newly-manufactured legacy helicopters, while minimizing the negative effects on OEMs and operators. (ROPWG, 2018, p.28)

Research Objective

In 2018, the Rotorcraft Occupant Protection Working Group (ROPWG) made recommendations to reduce blunt force trauma using Crash Resistant Seating Systems. These recommendations included changes to §27/29.562 such as changing the load factors used for testing to show compliance. The recommendations made by the ROPWG would not be for full compliance to the dynamic seat rule, thus the FAA needs to evaluate the safety benefit and decide if they would meet the safety intent of the current rule for retrofit and new manufacturing of existing type design.

[1]The ARAC Task 5 report referred to the 1989 Crash Survival Design Guide (CSDG), but we could not locate these values in the CSDG. Instead, we found the information in the Analysis of Rotorcraft Crash Dynamics for Development of Improved Crashworthiness Design Criteria.

To evaluate the recommendations of the ROPWG, the FAA needs data for specific emergency landing conditions. The data will be used to determine if updates are recommended for the applicable advisory circulars and prepare for any potential future rulemaking activity. The research was split into three phases:

1. An evaluation of the five most common rotorcraft in the US civilian fleet to determine the baseline floor and restraint attachment strength of rotorcraft in the flying fleet and recommend incremental improvements to make them safer. This work was conducted by a consultant.
2. An evaluation of impact pulse versus seat stroke using a rigid seat.
3. Cooperative research between Civil Aerospace Medical Institute (CAMI) and National Aeronautics and Space Administration (NASA) Langley Research Center to obtain data supporting development and evaluation of overhead-structure interaction with rotorcraft seats and restraints systems.

This paper reports on the results of the second phase of the research. While analyzing the correlation between seat stroke and lumbar load, an opportunity was taken to explore potential correlations for lumbar load versus pelvis acceleration, lumbar load versus seat-pan acceleration, seat-pan acceleration versus seat stroke distance, and if pelvic acceleration could replace lumbar load as a determinant of occupant injury potential.

Methods

To meet the occupant injury limits, rotorcraft seats must be designed to absorb energy. To evaluate these parameters, the Biodynamics Team at CAMI built a Reusable Energy Attenuating Laboratory (REAL) Seat using the United States Navy's design. This seat design allowed the researchers to vary the seat stroke distance and compare it to the loads transmitted to the occupant.

Reusable Energy Attenuating Laboratory (REAL) Seat

Sled Mounted Components

The REAL Seat's sled mounted components consist of the structural supports, pitch plate, linear rails, brake system (pneumatic accumulator), floor structure, and emergency load limiter (*Figure 1*). The structural supports are two welded I-beam triangles (30°, 60°, and 90°) which are mounted to the CAMI impact sled's top plate. The pitch plate was mounted to the structural supports 30° off horizontal, this angle replicates the pitch defined in the 2X.562 vertical test condition. Attached to the pitch plate were the linear rails, the brake accumulator, and the floor support structure. The floor sub-structure provided the mounting surface for a 6-axis load cell and floor pan (*Figure 2*). An aluminum honeycomb panel was used as an emergency load limiter, to protect the seat system in the event of brake system failure.

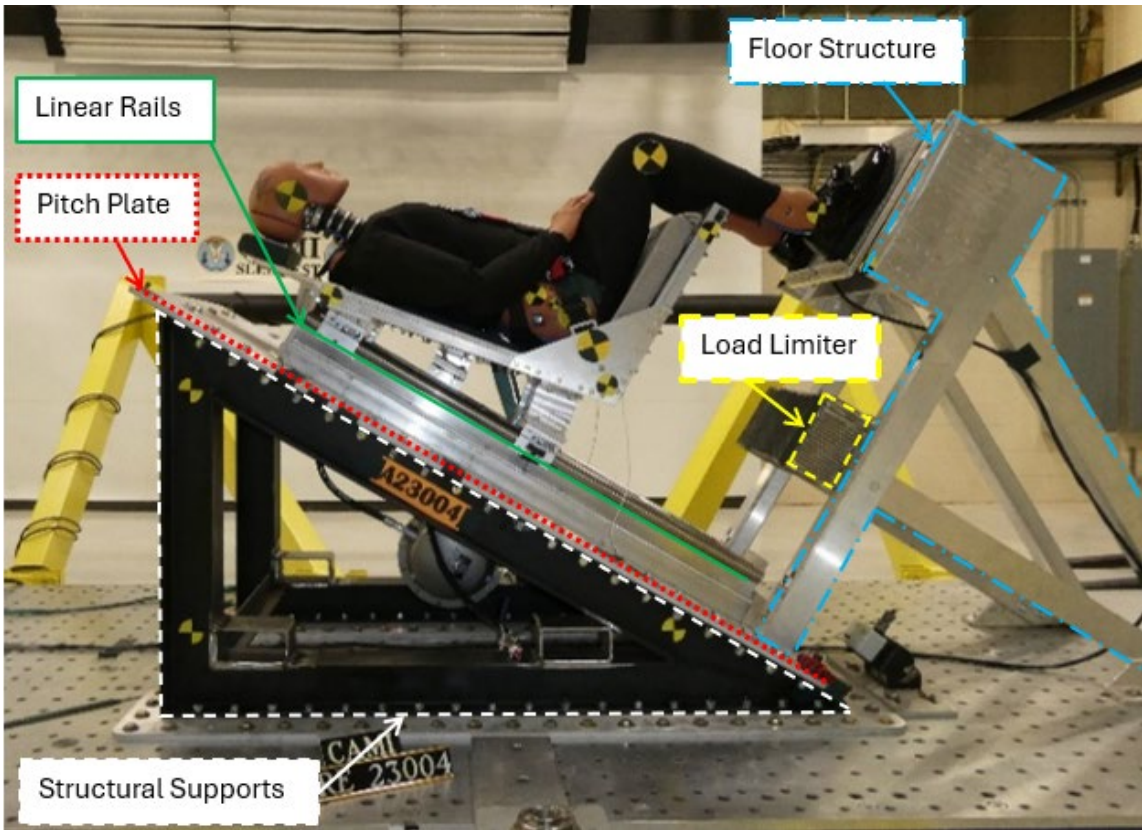

Figure 1: Side View of the REAL Seat Mounted on CAMI Sled (Accumulator Not Highlighted).

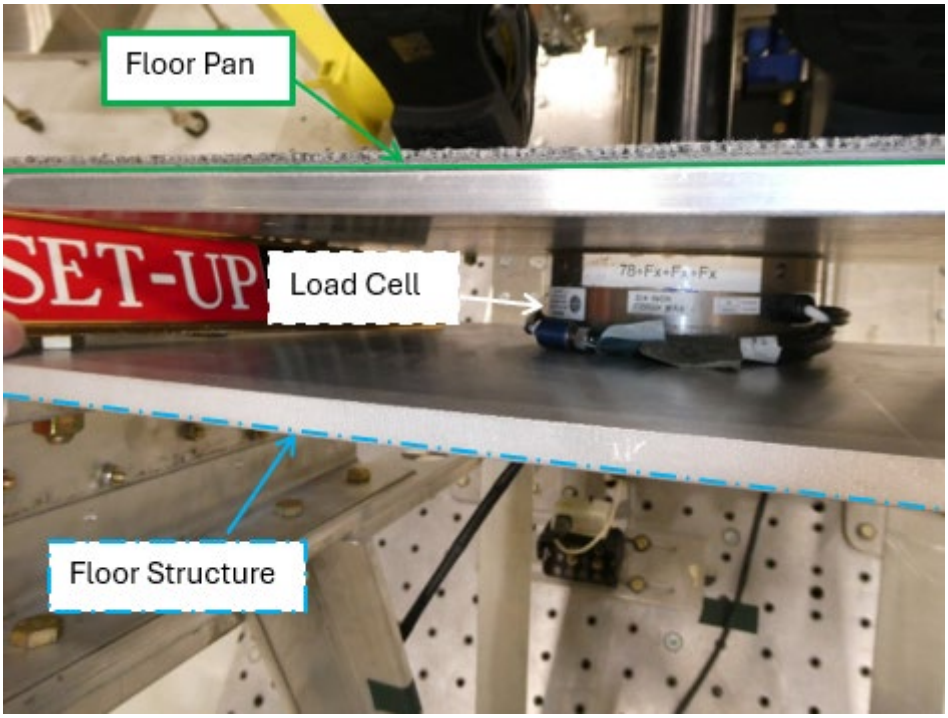

Figure 2: Front View of the Load Cell Mounted Between Floor Structure and Floor Pan.

The seat bucket is the segment of the REAL Seat that moves along the linear rails, allowing for testing of different seat strokes. It comprises the seat back, seat pan, brake blade, seat pan cushion, five-point harness, and four linear bearings, which constrain the seat motion along the linear rails. The maximum stroke the system can achieve is approximately 18 in. The plates used for the seat back and pan are half-inch thick aluminum plate, with the seat back angled 10° rearward from vertical. The brake blade is mounted directly to the structure of the seat bucket behind the seat back. *Figure 3* shows the two lower linear-bearing attachment points, brake blade, braking system, and linear rails. The seat pan cushion was a 2 in. blue Confor™ 45 AC foam covered in 100% cotton fabric. A seat back cushion was not included in the testing. The occupant restraint was a five-point Nylon harness. A string potentiometer was mounted between the seat bucket and the support structure to measure seat stroke distance during the event. Two accelerometers were mounted underneath the seat pan, at each rear corner, to measure seat pan acceleration, providing redundancy.

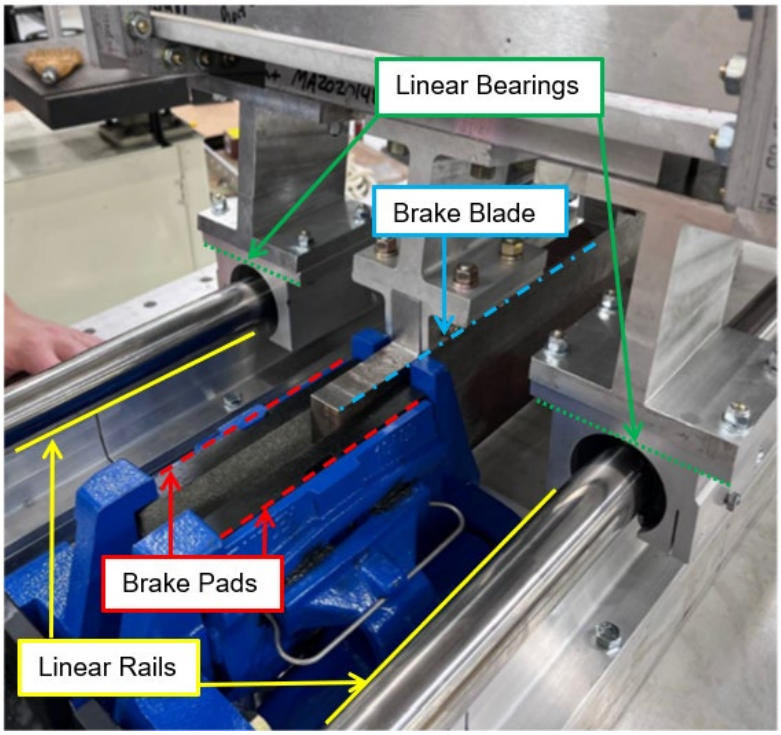

Figure 3: REAL Seat Linear Rails and Brake System.

Operation

The integrated brake system uses pneumatic pressure to control the seat stroking force. The system has a maximum operating pressure of 100 pounds per square inch (psi). Based on a given sled acceleration, seat bucket weight, and anthropometric test device (ATD) weight, the pressure required for a nominal seat stroke distance can be determined. The Navy provided a calculator to predict seat-stroke based on desired occupant acceleration, ATD weight, and additional equipment weight in the seat bucket, such as helmets and aircrew equipment. However, differences in seat orientation, such as pitch and roll, between the CAMI and Navy seats resulted

in performance differences and necessitated additional checks to quantify the CAMI REAL Seat performance.

Over 90 initialization runs were conducted to verify operation of the REAL Seat. The first 20 tests were used to burnish the brake pads, ensuring that stroke characteristics remained consistent as the brake blade and pads underwent repeated cycles. The remaining tests were used to determine the relationship between pressure and seat stroke based on the sled acceleration and the total payload (seat plus ATD). An external air supply was used to fill the brake accumulator immediately after the ATD was positioned. The accumulator was pressurized to set the brakes, followed by final pretest checks and photographs which required approximately 10-15 minutes to complete. Immediately prior to arming the sled, the brake pressure was verified and pressure increased if necessary. The seat stroke was measured based on the difference between the pretest and posttest seat positions in the seat coordinate system using a tape measure. At the completion of the 90 initialization runs, it was observed that the repeatability of seat stroke distance for a set pressure was ± 1 in. During these runs, the seat was not instrumented with a potentiometer. Given the seat stroke variation for a set pressure was approximately 2 inches, the use of highly precise measurement instruments, such as a coordinate measuring machine (CMM), was considered unnecessary for pretest and posttest measurements.

Anthropomorphic Test Device

The 50th percentile FAA-Hybrid III ATD was used to assess injury risk. This ATD is a modification of the automotive Hybrid III to incorporate parts of the Hybrid II to make it acceptable for aviation testing (Gowdy, et. al., 1999). *Figure 1* shows the FAA-Hybrid III ATD in the REAL Seat.

ATD Seating Method

The nominal upright ATD seated position (1-g position) was determined with respect to rigid points on the REAL Seat. A surrogate wooden seat with pan and back angles identical to the REAL seat was used to determine the 1-g position (*Figure 4*). The height of the floor pan was set so the vertical distance between the Anthropomorphic Test Device's (ATD) hip point (H-point) and ankle was approximately 13 in. in the seat coordinate system (for both the Wooden 1-g seating fixture and the REAL Seat), see *Figure 4*. 13 in. is the standard distance CAMI uses for tests with a rigid seat. This distance typically provides some clearance between the distal portion of the thigh and the seat cushion and is similar to the height achieved for a standard transport category economy seat. The ATD was seated following the guidance in AS8049D (SAE International 8049D) which involves lowering the ATD into the seat while holding the thighs horizontally and pushing the ATD rearward with approximately 20 lb. of force. This resulted in a consistent fore/aft position and initial pelvis angle (Moorcroft, et. al., 2010). Markers were placed on the ATD pelvis at the projection of the H-point, an auxiliary target 3 in. directly above that point (vertical H-point target), at the head center of gravity (CG), and knee center target. A three-dimensional CMM was then used to record the photometric target locations. The pelvis angle was derived based on the H-point and vertical H-point and torso angle was derived based on a line between the head CG and H-point. The average location of the ATD H-point, vertical H-point and head CG from the 1-g seating was used to define the goals for the vertical seating.

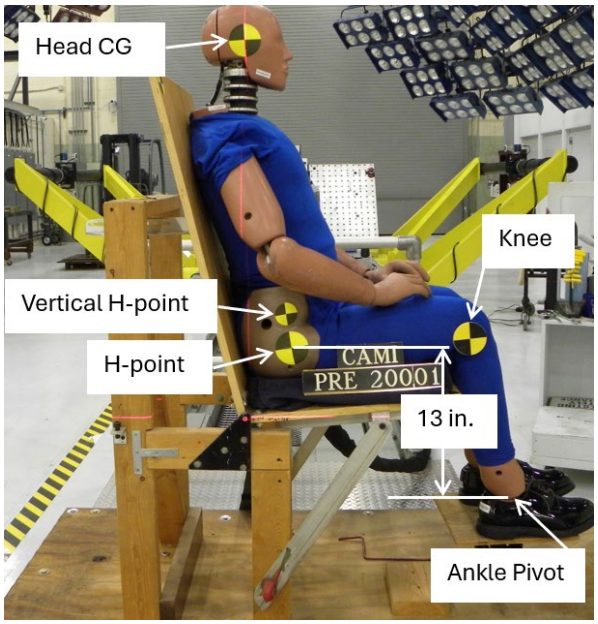

Figure 4: FAA Hybrid III on Wooden 1-g Seating Fixture.

Test Pulses

Three input pulses were chosen for this series with acceleration peaks of 25 g, 27.5 g, and 30 g. All three pulses are triangular shaped with the same onset rate based on the Part 2X.562 input pulse (*Figure 5*). The total pulse duration is slightly longer than twice the rise time to ensure the velocity requirement was met. The 30 g pulse is defined by Part 2X.562, the 27.5 g pulse is defined by the ARAC report, and the 25 g pulse was selected as an additional test condition to evaluate a lower test severity. *Table 1* lists the three pulses with their minimum velocity change, minimum peak acceleration, rise time, and total duration.

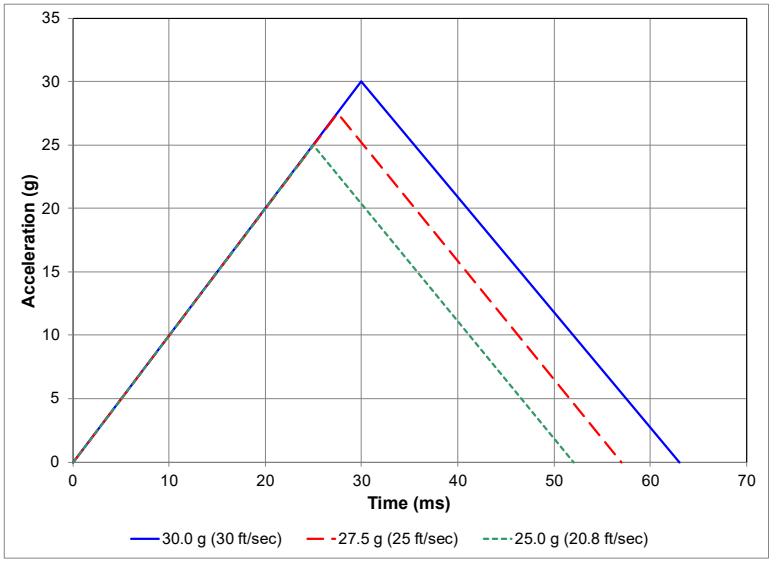

Figure 5: Input Pulses.

Table 1: Input Acceleration Pulses.

Min Velocity Change (ft/sec)	Min Peak (g)	Rise Time (ms)	Total Duration (ms)
30	30	30	63
25	27.5	27	57
20.8	25	25	52

Instrumentation

Electronic Instrumentation

The instrumentation of the sled, ATD, and seat collected for this project are shown in *Table 2*. The test data were gathered and filtered per the requirements of SAE J211-1 (SAE International, 2022a). The sign convention of the recorded signals conformed to SAE J1733 (SAE International, 2024). Some data sets present the normalized lumbar load, which is calculated by dividing the target peak acceleration by the actual peak acceleration and then multiplying it by the measured lumbar load. This adjustment compensates for small differences in peak sled acceleration when comparing results (Deweese, et. al., 2021). This procedure is acceptable in accordance with Aerospace Standard 8049 (SAE International 8049D).

Table 2: Instrumentation List.

Description	Units	Filter Class
Sled Acceleration	g	60
Seat Pan Acceleration	g	60
Pan Displacement	in.	180
Head Acceleration (A_x, A_y, A_z)	g	1000
Upper Neck Loads (F_x, F_y, F_z)	lb.	1000
Upper Neck Moments (M_x, M_y, M_z)	in.-lb.	600
Lumbar Force (F_x, F_y, F_z)	lb.	600
Lumbar Moment (M_x, M_y, M_z)	in.-lb.	600
Spinal Acceleration (A_x, A_y, A_z)	g	180
Pelvis Acceleration (A_x, A_y, A_z)	g	1000

Video Coverage

Color high-speed video was collected at 1,000 frames per second with a 1174 x 1196 resolution. The video was captured from each side of the impact sled, perpendicular to direction of travel. The positions of selected targeted points were measured initially with a CMM and derived during the test from the videos using procedures complying with the requirements of SAE J211-2 (SAE International, 2022b). Quadrant targets were placed on the ATD at the head center of gravity, knee, ankle, the side of the pelvis at the H-point, a vertical pelvis location above the H-point, and aft of the vertical H-point target (*Figure 4*). Targets were also placed on the REAL Seat structures for scaling and capturing relative movement.

Test Matrix

Forty-eight tests were conducted. *Table 3* summarizes the test matrix for the 48 tests conducted, indicating nominal seat-stroke length and the sled input-pulse peak acceleration. The run numbers are based on the standard CAMI naming convention; dynamic impact tests are labeled with an 'A,' the year of the run is recorded using two digits, and the next three numbers indicate the chronological order for the run within that year. For example, the first dynamic test for 2023 is designated A23001.

Table 3: Test Matrix.

Nominal Seat Stroke (in.)	30 g Pulse	27.5 g Pulse	25 g Pulse
1	-	-	A23048
1	-	-	A23049
1	-	-	A23050
2	A23003	A23009	A23027
2	A23004	A23010	A23034
2	A23005	A23011	A23035
4	A23036	A23012	A23033
4	A23037	A23013	A23028
4	A23038	A23014	A23029
6	A23039	A23015	A23030
6	A23040	A23016	A23031
6	A23041	A23017	A23032
8	A23045	A23018	A23006
8	A23046	A23019	A23007
8	A23047	A23020	A23008
10	A23042	A23021	A23024*
10	A23043	A23022	A23025*
10	A23044	A23023	A23026*

**Tests were run with a modified 25 g pulse, where the rise time was 50 ms and the velocity change was ~40 ft/sec.*

RESULTS

Input Pulses

Figure 6 shows representative achieved pulse for each test pulse.

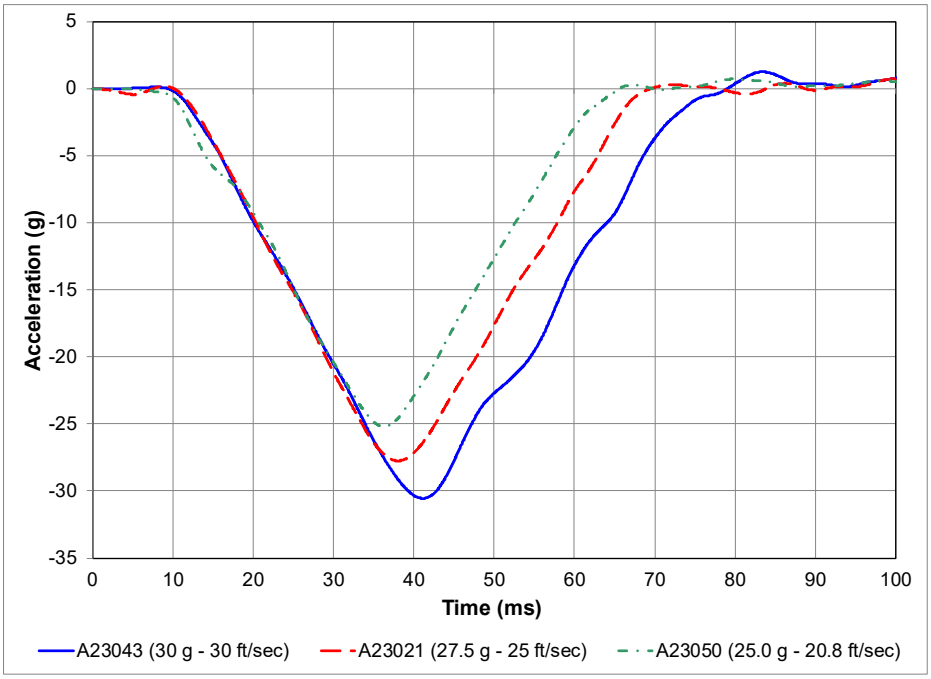

Figure 6: Example of Each Achieved Pulses.

Data Summary

Tables 4-7 contain a summary of the seat stroke, peak acceleration, and loads split by their respective input pulses. The data for the 30 g pulse is detailed in *Table 4*, the 27.5 g pulse data is in *Table 5*, and the 25 g pulse data is in *Table 6*. Three 25-g tests were conducted with an extended duration (long duration 25 g) due to an input discrepancy; the anomalous pulse had a time-to-peak of 38 ms and a total time of 78 ms, and the results are reported in *Table 7*.

The seat stroke distance values include the nominal (goal) seat stroke and the measured. The peak acceleration values include the sled, ATD pelvis in the Z-direction and seat pan in the Z-direction. The load data includes the peak lumbar in Z-direction, normalized lumbar load, and peak floor load in Z-direction.

Table 4: 30-g Data Summary.

Test #	Nominal Seat Stroke (in.)	Measured Seat Stroke (in.)	Achieved (g)	Peak Pelvis Acceleration in Z (g)	Peak Seat Pan Acceleration (g)	Lumbar Load in Z (lb.)	Normalized Lumbar Load (lb.)	Floor Load in Z (lb.)
A23003	2	1.45	-31.6	-31.1	-26.0	-2675	-2540	2324
A23004	2	1.25	-31.4	-30.0	-24.9	-2586	-2471	2180
A23005	2	1.25	-31.5	-32.9	-25.2	-2673	-2546	2110
A23036	4	3.35	-30.3	-28.7	-19.9	-2057	-2037	2132
A23037	4	4.45	-30.3	-23.4	-17.6	-1734	-1717	1996
A23038	4	3.95	-30.2	-26.3	-18.5	-1908	-1895	2133
A23039	6	6.45	-30.8	-19.9	-15.2	-1387	-1351	2084
A23040	6	6.05	-31.4	-20.4	-18.4	-1380	-1318	2074
A23041	6	6.00	-31.8	-21.0	-16.6	-1479	-1395	2066
A23045	8	7.50	-30.7	-15.7	-16.7	-1131	-1105	2101
A23046	8	7.70	-30.2	-16.6	-16.4	-1154	-1146	2060
A23047	8	8.35	-30.7	-15.8	-14.4	-1072	-1048	2166
A23042	10	9.35	-31.6	-14.6	-16.4	-1000	-949	2154
A23043	10	10.65	-30.6	-13.9	-13.8	-931	-913	2169
A23044	10	9.65	-30.7	-15.7	-13.4	-917	-896	2095

Table 5: 27.5-g Data Summary.

Test #	Nominal Seat Stroke (in.)	Measured Seat Stroke (in.)	Achieved (g)	Peak Pelvis Acceleration in Z (g)	Peak Seat Pan Acceleration (g)	Lumbar Load in Z (lb.)	Normalized Lumbar Load (lb.)	Floor Load in Z (lb.)
A23009	2	2.45	-29.2	-24.7	-24.0	-1818	-1712	2235
A23010	2	2.00	-27.6	-26.1	-20.3	-1896	-1889	2322
A23011	2	1.50	-27.9	-28.2	-26.8	-2167	-2135	2260
A23012	4	3.15	-27.7	-22.0	-18.1	-1560	-1549	2237
A23013	4	3.95	-27.6	-19.8	-15.4	-1364	-1359	2153
A23014	4	4.00	-27.8	-18.7	-15.3	-1338	-1324	2230
A23015	6	4.95	-27.7	-18.9	-13.7	-1255	-1246	2284
A23016	6	5.65	-27.5	-15.8	-13.7	-1132	-1132	2144
A23017	6	6.45	-27.7	-15.5	-13.5	-1051	-1043	2244
A23018	8	8.80	-27.9	-11.4	-11.2	-775	-764	2079
A23019	8	9.00	-28.3	-12.8	-12.6	-797	-774	2155
A23020	8	7.90	-28.0	-12.1	-13.8	-828	-813	2230
A23021	10	11.15	-27.8	-12.4	-10.7	-700	-692	2310
A23022	10	10.85	-28.0	-11.7	-13.5	-686	-674	2112
A23023	10	10.05	-27.2	-12.0	-11.0	-671	-616	2116

Table 6: 25-g Data Summary.

Test #	Nominal Seat Stroke (in.)	Measured Seat Stroke (in.)	Achieved (g)	Peak Pelvis Acceleration in Z (g)	Peak Seat Pan Acceleration (g)	Lumbar Load in Z (lb.)	Normalized Lumbar Load (lb.)	Floor Load in Z (lb.)
A23048	1	0.25	-24.8	-31.3	-20.8	-2271	-2289	1977
A23049	1	0.40	-24.4	-30.8	-21.2	-2127	-2179	2007
A23050	1	0.75	-25.2	-30.0	-19.3	-2128	-2111	1947
A23027	2	3.00	-25.4	-17.1	-17.8	-1168	-1149	2156
A23034	2	2.15	-25.4	-19.4	-15.0	-1361	-1338	2020
A23035	2	1.95	-25.1	-20.5	-15.1	-1416	-1410	2071
A23033	4	3.35	-25.5	-17.7	-17.4	-1190	-1167	2142
A23028	4	4.35	-25.0	-14.6	-11.8	-907	-907	2153
A23029	4	4.05	-24.4	-14.9	-12.3	-962	-986	2043
A23030	6	5.60	-24.9	-12.4	-11.2	-741	-744	2127
A23031	6	6.25	-25.4	-11.8	-17.3	-758	-746	2230
A23032	6	6.15	-25.3	-12.6	-11.0	-759	-750	2204
A23006	8	8.00	-25.9	-10.4	-10.2	-608	-587	2161
A23007	8	8.65	-26.4	-11.5	-11.2	-649	-615	2416
A23008	8	8.50	-26.2	-9.8	-10.2	-636	-607	2285

Table 7: Long Duration 25-g Data.

Test #	Nominal Seat Stroke (in.)	Measured Seat Stroke (in.)	Achieved (g)	Peak Pelvis Acceleration in Z (g)	Peak Seat Pan Acceleration (g)	Lumbar Load in Z (lb.)	Normalized Lumbar Load (lb.)	Floor Load in Z (lb.)
A23024	10	10.25	-25.1	-13.4	-12.0	-810	-807	1498
A23025	10	10.05	-25.9	-13.2	-11.4	-904	-873	1299
A23026	10	9.65	-25.5	-14.1	-15.1	-925	-907	1294

Figure 7, *Figure 8*, and *Figure 9* show time history plots of sled acceleration, pelvis acceleration in the Z-direction, and lumbar load in the Z-direction from three of the 30 g tests to show the typical shapes.

- *Figure 7* (A23043 - 10 in. stroke), maximum sled acceleration of -30.5 g at 41 ms, pelvis acceleration of -13.9 g at 47 ms, and a lumbar load of -931 lb. at 54 ms.
- *Figure 8* (A23040 – 6 in. stroke) maximum sled acceleration of -31.4 g at 42 ms, pelvis acceleration of -20.4 g at 46 ms, and lumbar load of -1380 lb. at 54 ms.
- *Figure 9* (A23004 – 2 in. stroke) maximum sled acceleration of -31.4 g at 41 ms, pelvis acceleration of -30.0 g at 47 ms, and lumbar load of -2586 lb. at 55 ms.

Notably, all tests show a spike in pelvis acceleration preceding the lumbar load peak, which aligns with a local minimum in pelvis acceleration, consistently occurring approximately 8 milliseconds apart, regardless of seat stroke length. Data from the 25-g and 27.5-g tests exhibit similar trends.

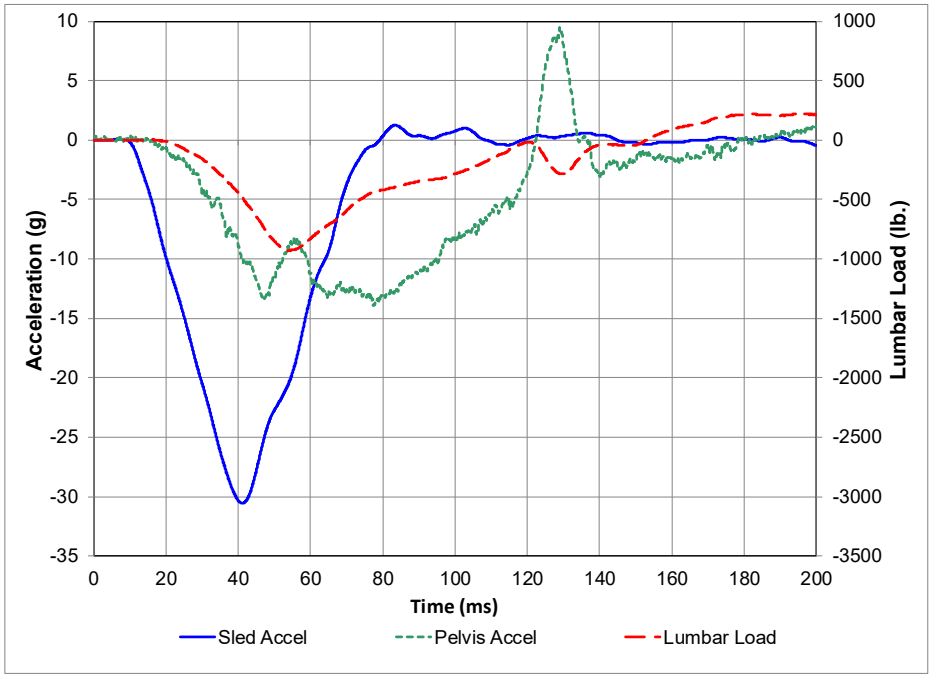

Figure 7: Sled Acceleration, Pelvis Acceleration and Lumbar Load for 30 g at 10 in. Seat Stroke (A23043).

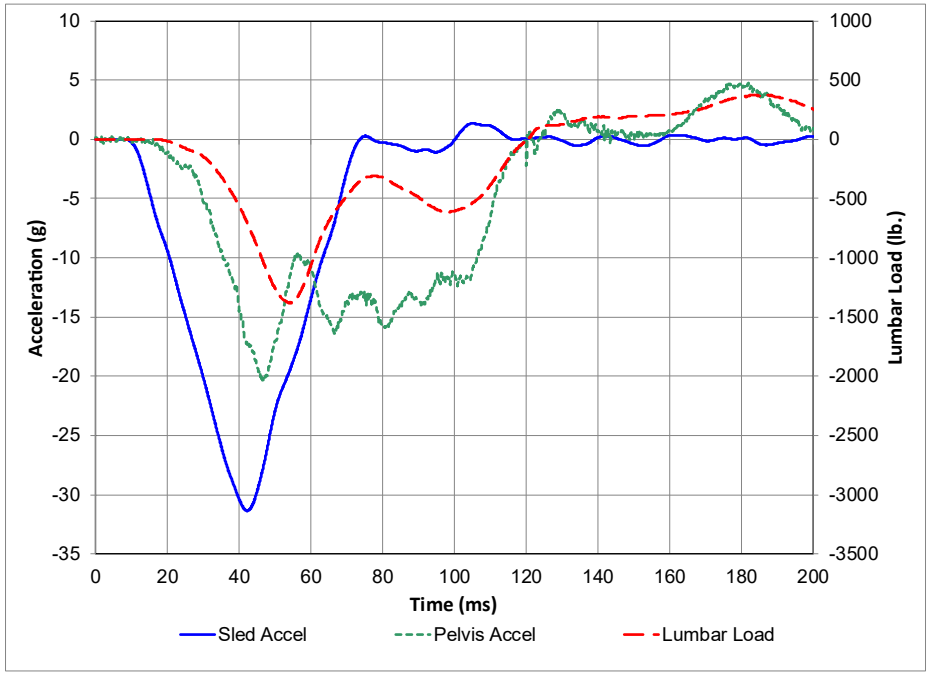

Figure 8: Sled Acceleration, Pelvis Acceleration and Lumbar Load for 30 g at 6 in. Seat Stroke (A23040).

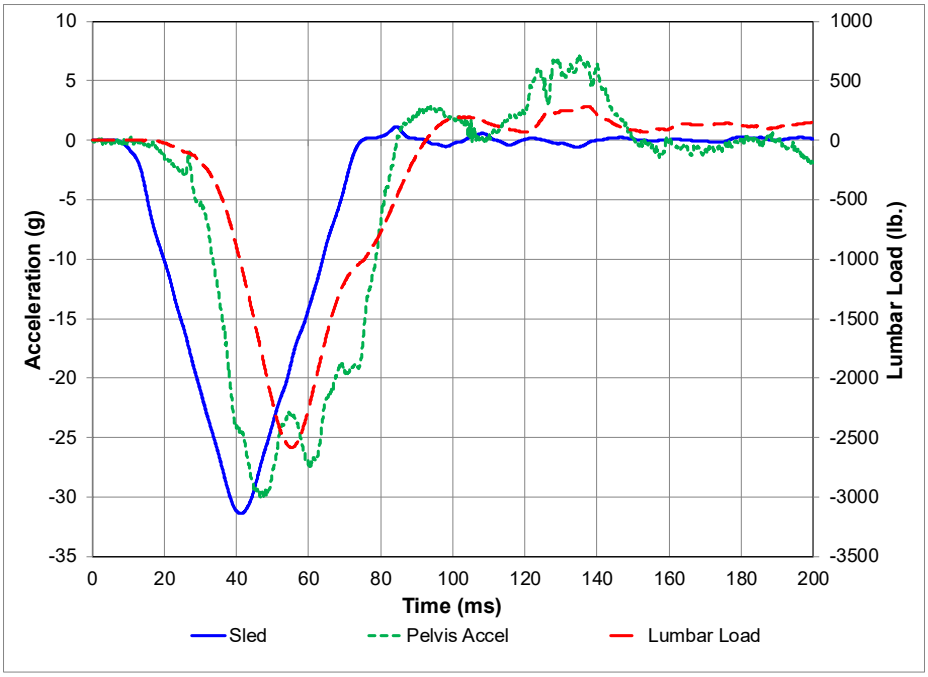

Figure 9: Sled Acceleration, Pelvis Acceleration and Lumbar Load for 30 g at 2 in. Seat Stroke (A23004).

Lumbar Load versus Seat Stroke Distance

Figure 10 compares normalized lumbar load (absolute value) against achieved seat stroke distance for each input pulse (30g, 27.5 g, 25 g). The data is grouped according to specific pulses, and normalization ensures that the values are comparable across the prescribed sled pulses. A natural logarithmic trendline provided the best fit for each pulse. Based on the trendlines, and the 1500 lb. lumbar load limit defined in 14 CFR § 2X.562, the estimated minimum stroke to remain below the 1500 lb. limit is at least 4.9 in. for a 30 g pulse, 3.4 in. for the 27.5 g pulse, and 1.4 in. for the 25 g pulse.

The trend line equation for the 30-g data (R^2=0.9739) is:

$$Lumbar\ Load\ = -803.4 * ln(Stroke) + 2781.7$$ *(Equation 1)*

The trend line equation for the 27.5-g data (R^2=0.9942) is:

$$Lumbar\ Load\ = -734.0 * ln(Stroke) + 2392.1$$ *(Equation 2*

The trend line equation for the 25-g data (R^2=0.9815) is:

$$Lumbar\ Load\ = -514.5 * ln(Stroke) + 1689.3$$ *(Equation 3)*

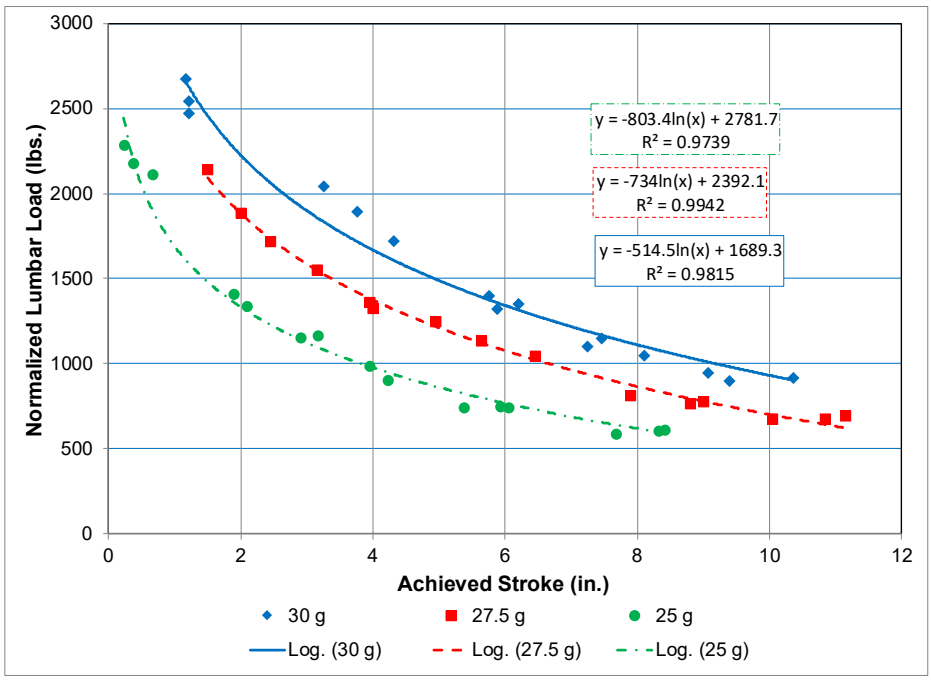

Figure 10: Normalized Lumbar Load versus Stroke Distance for 25-g, 27.5-g, and 30-g Pulses.

Lumbar Load versus Pelvis Acceleration

Figure 11 plots the measured lumbar load (absolute value) versus pelvis acceleration in the Z-direction for each input pulse. Normalization of the lumbar load to the achieved sled pulse was not calculated for this section since the goal was to establish a correlation between the lumbar load and pelvis acceleration which does not have a normalization procedure. A linear trend line provided the best fit for the three data sets, while not being forced through (0,0)[2].

The equation for the linear trend line for the 30-g data (R^2=0.9460) is :

$$Lumbar\ Load\ = 91.955 * Pelvis\ Acceleration - 402.12 \quad \textit{(Equation 4)}$$

The equation for the linear trendline for the 27.5-g data (R^2=0.9871) is:

$$Lumbar\ Load\ = 84.542 * Pelvis\ Acceleration - 274.5 \quad \textit{(Equation 5)}$$

The equation for the linear trendline for the 25 g-data (R^2=0.9953) is:

$$Lumbar\ Load\ = 77.041 * Pelvis\ Acceleration - 180.97 \quad \textit{(Equation 6)}$$

Using the trendline equations from *Figure 11* and setting the Y-value (lumbar load) to 1500 lb., the pelvis acceleration is calculated as follows: 20.7 g (30-g trendline), 21.0 g (27.5-g trendline), and 21.8 g (25-g trendline).

[2] Appendix A provides a discussion of the equations used for the linear trendlines.

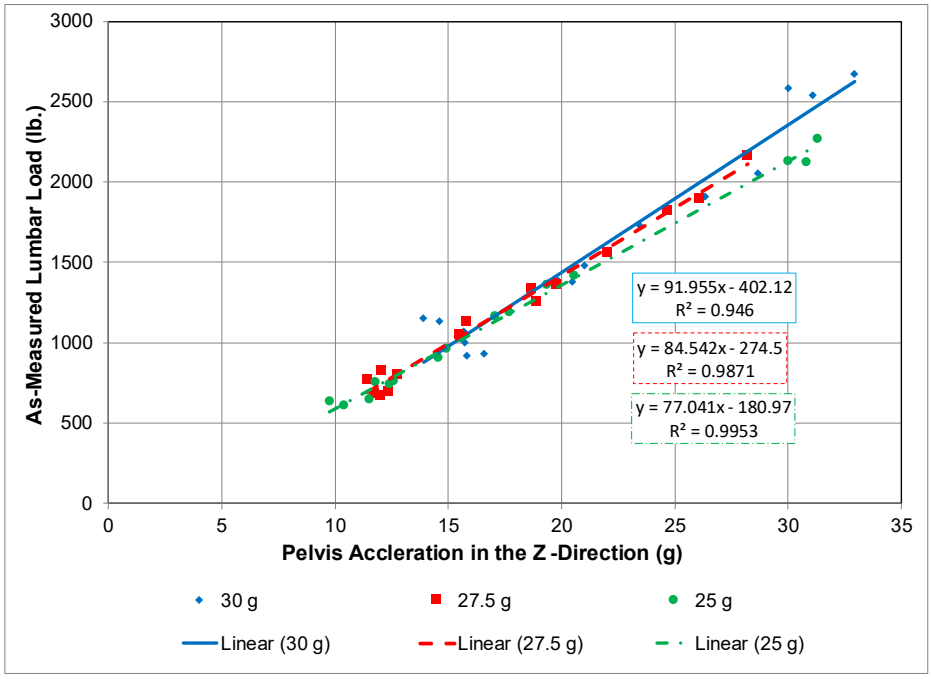

Figure 11: Lumbar Load versus Pelvis Acceleration for 25-g, 27.5-g and 30-g Pulses.

Due to significant overlap observed across the lumbar load versus pelvis acceleration data, the datasets were combined into a single data series (***Figure 12***). A linear trend line was found to provide the best fit for the combined dataset. This suggests the lumbar load is linearly correlated to the pelvis acceleration and is independent of the sled input pulse for this stroking seat and this range of sled pulses. These results are consistent to previous work by the military and is discussed in the *Spinal Injury Risk section*.

The equation of the combined data trendline (R^2=0.9685) is:

$$Lumbar\ Load\ = 84.938 * Pelvis\ Acceleration - 283.78 \quad \textit{(Equation 7)}$$

Based on this trendline equation, the pelvis acceleration must remain below 21.0 g to ensure that the lumbar load does not exceed the 1,500 lb. limit specified in §2X.562. For improved visualization, ***Figure 13*** presents a combined plot of the three trendlines from ***Figure 11*** along with the trendline for the combined data from ***Figure 12***.

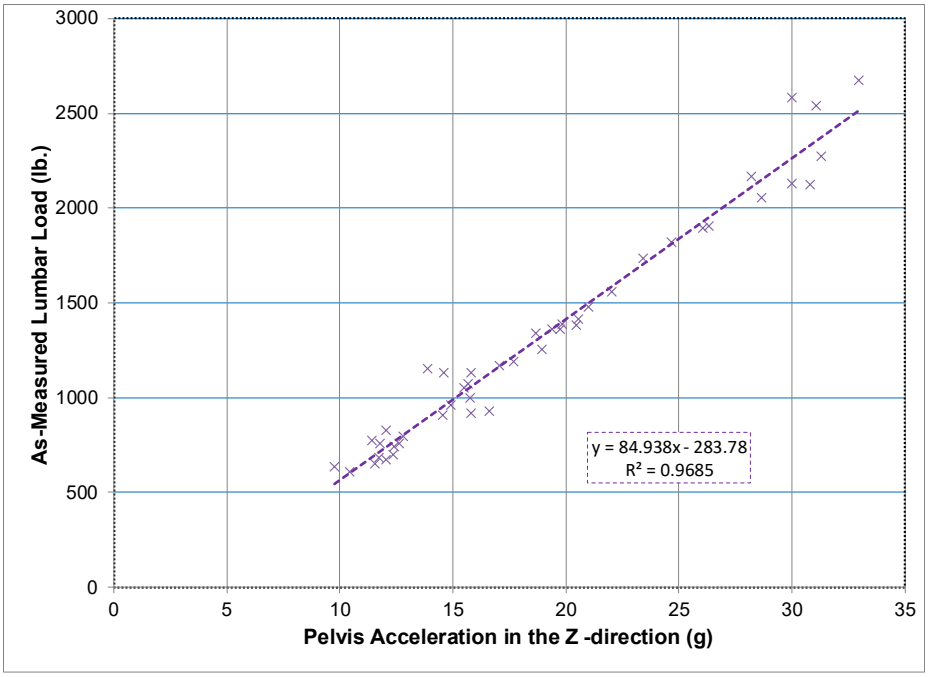

Figure 12: Lumbar Load versus Pelvis Acceleration in a Single Data Set.

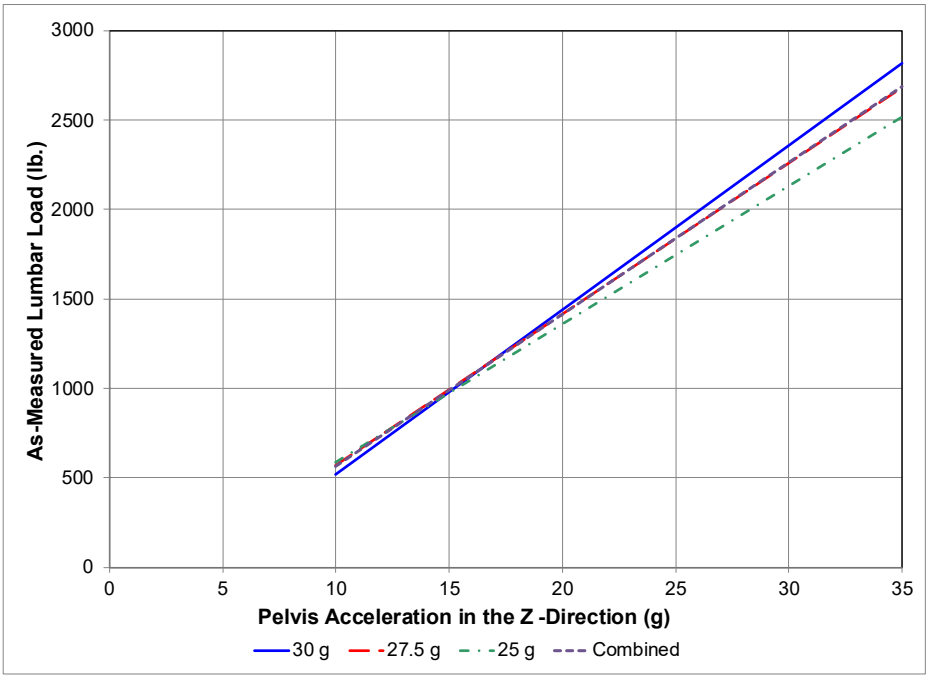

Figure 13: Trendlines from the Four Lumbar Load versus Pelvis Acceleration Trendlines.

Lumbar Load versus Seat Pan Acceleration

The as-measured lumbar load plotted against seat pan acceleration for the three separate pulse datasets is presented in ***Figure 14***. Each dataset, for the range of accelerations tested, is best represented by a linear trend line. As with the lumbar load versus pelvis acceleration in the Z-direction, the three datasets were combined into a single dataset (***Figure 15***). A linear trend line

also provided the best fit for this combined dataset. From that trend line (Equation 11), the lumbar load remains below the 1500 lb. regulatory limit when the seat-pan acceleration remains below 17.6 g, irrespective of the input pulse. This derived limit is consistent with the Department of Defense Joint Service Specification Guide (JSSG) (Department of Defense, 1999), which requires that occupants "shall not be subjected to a peak vertical load factor greater than 20 g," with the aircraft structure designed so that progressive failure limits the vertical load factor at the seat to 20 g. Thus, the 17.6 g threshold derived here lies within the JSSG structural crashworthiness constraint.

The equation for the linear trend line for the 30-g data (R^2=0.8565) is:

$$Lumbar\ Load\ = 139.98 * Seat\ Acceleration - 954.23 \quad \textit{(Equation 8)}$$

The equation for the linear trendline for the 27.5-g data (R^2=0.8773) is:

$$Lumbar\ Load\ = 94.92 * Seat\ Acceleration - 272.92 \quad \textit{(Equation 9)}$$

The equation for the linear trendline for the 25 g-data (R^2=0.7512) is:

$$Lumbar\ Load\ = 134.56 * Seat\ Acceleration - 794.06 \quad \textit{(Equation 10)}$$

The equation for the linear trendline for the combined data (R^2=0.8352) is:

$$Lumbar\ Load\ = 121.27 * Seat\ Acceleration - 634.27 \quad \textit{(Equation 11)}$$

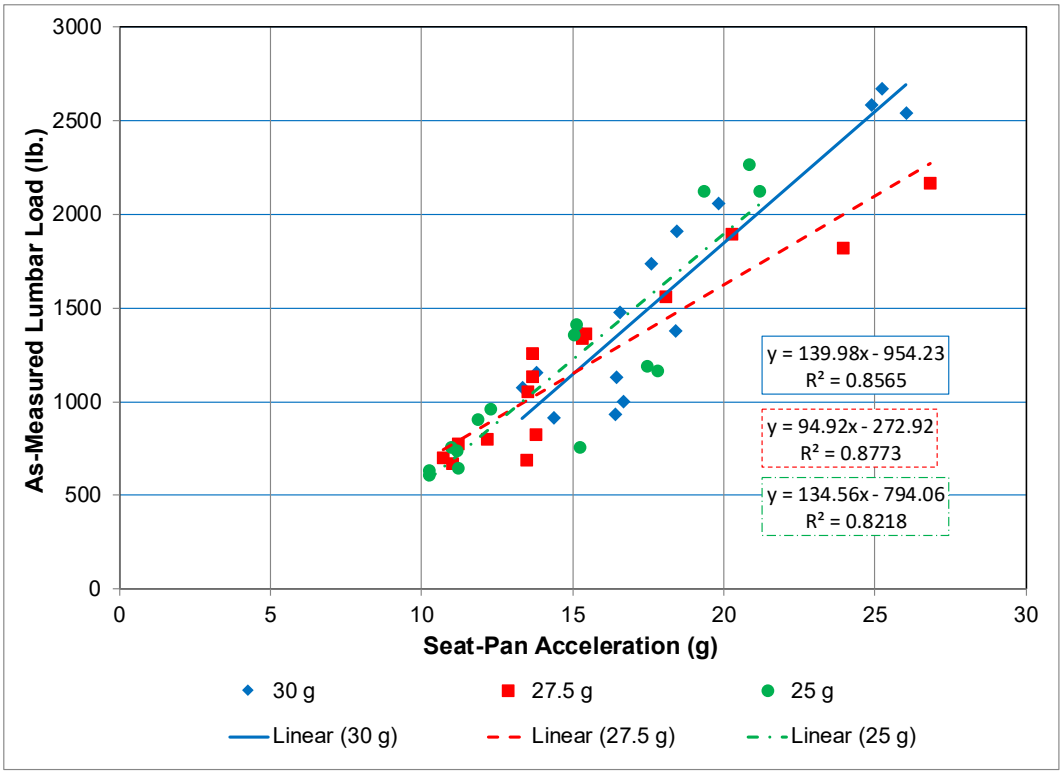

Figure 14: Lumbar Load versus Seat Pan Acceleration for 25-g, 27.5-g, and 30-g Pulses.

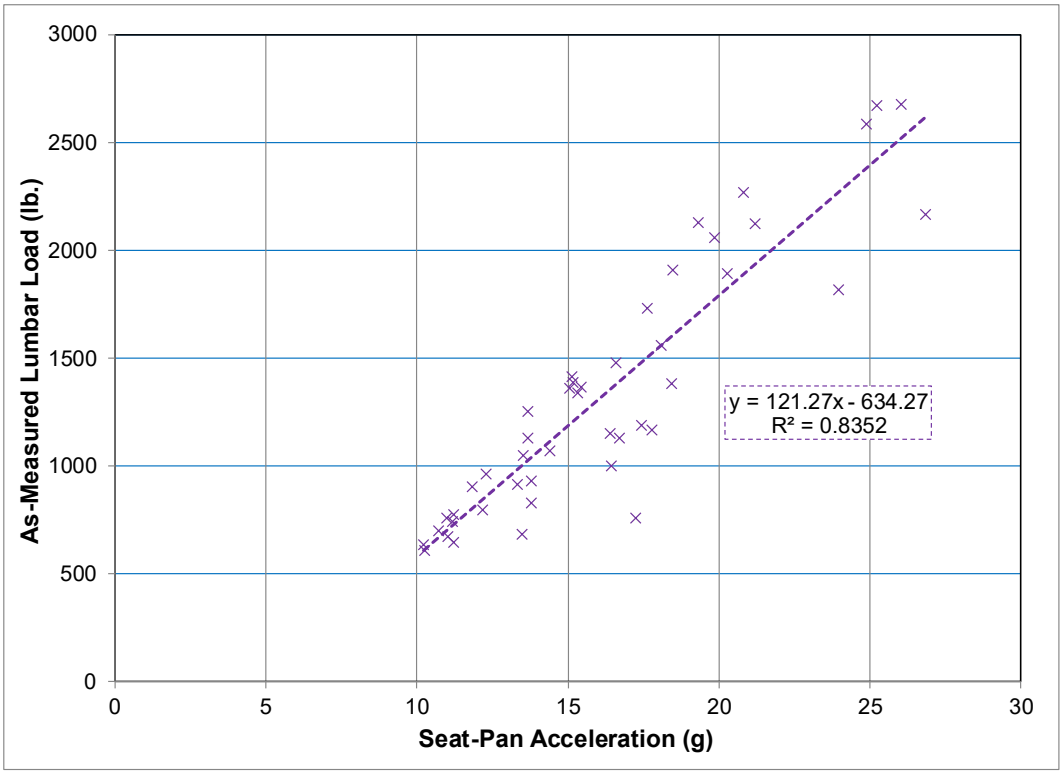

Figure 15: Lumbar Load versus Seat-Pan Acceleration for All Input Pulses.

Seat Pan Acceleration versus Seat Stroke

Seat-pan acceleration vs seat stroke was plotted for the three test pulses (*Figure 16)*. A natural-logarithmic trendline provided the best fit for each pulse data set.

The equation for the linear trendline for the 30-g data (R^2=0.9365) is:

$$Pan\ Acceleration\ = -5.358 * ln(Stroke) + 26.58$$ *(Equation 12)*

The equation for the linear trendline for the 27.5-g data (R^2=0.8495) is:

$$Pan\ Acceleration\ = -6.85 * ln(Stroke) + 26.795$$ *(Equation 13)*

The equation for the linear trendline for the 25-g data (R^2=0.7918) is:

$$Pan\ Acceleration\ = -3.111 * ln(Stroke) + 17.931$$ *(Equation 14)*

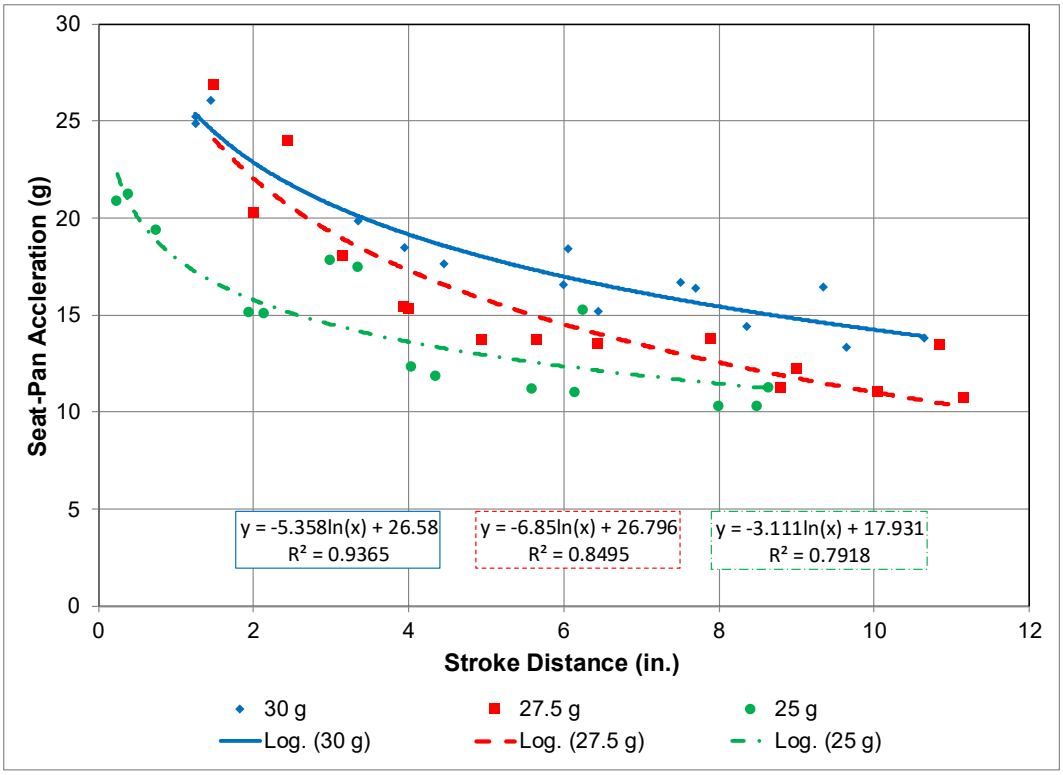

Figure 16: Stroke Distance vs Seat-Pan Acceleration for the 27.5-g Sled Pulse.

Kinematics

Test A23043 was selected as a representative example due to its kinematic similarity with the other tests in the series. This test was set up to achieve 10 in. of seat stroke with a 30 g pulse. *Figure 16* shows the ATD's position at 0, 54, 77, and 137 ms illustrating key kinematic stages: initial position, lumbar load peak (54 ms; seat stroke = 1.9 in.), peak pelvis acceleration (77 ms; seat stroke = 5.9 in.), and near-full stroke at 137 ms when the forward motion of the ATD was constrained by the upper torso restraints.

Due to the extensive neck bending seen in the videos, the neck injury criteria (N_{ij}) was calculated for all tests. The N_{ij} limit is 1.0. For the test shown in *Figure 17*, Nij was 0.320, well below the acceptance limit. The maximum Nij observed across the series was 0.351 (A32005, 30 g, 1.25 in. stroke), which remains under the threshold.

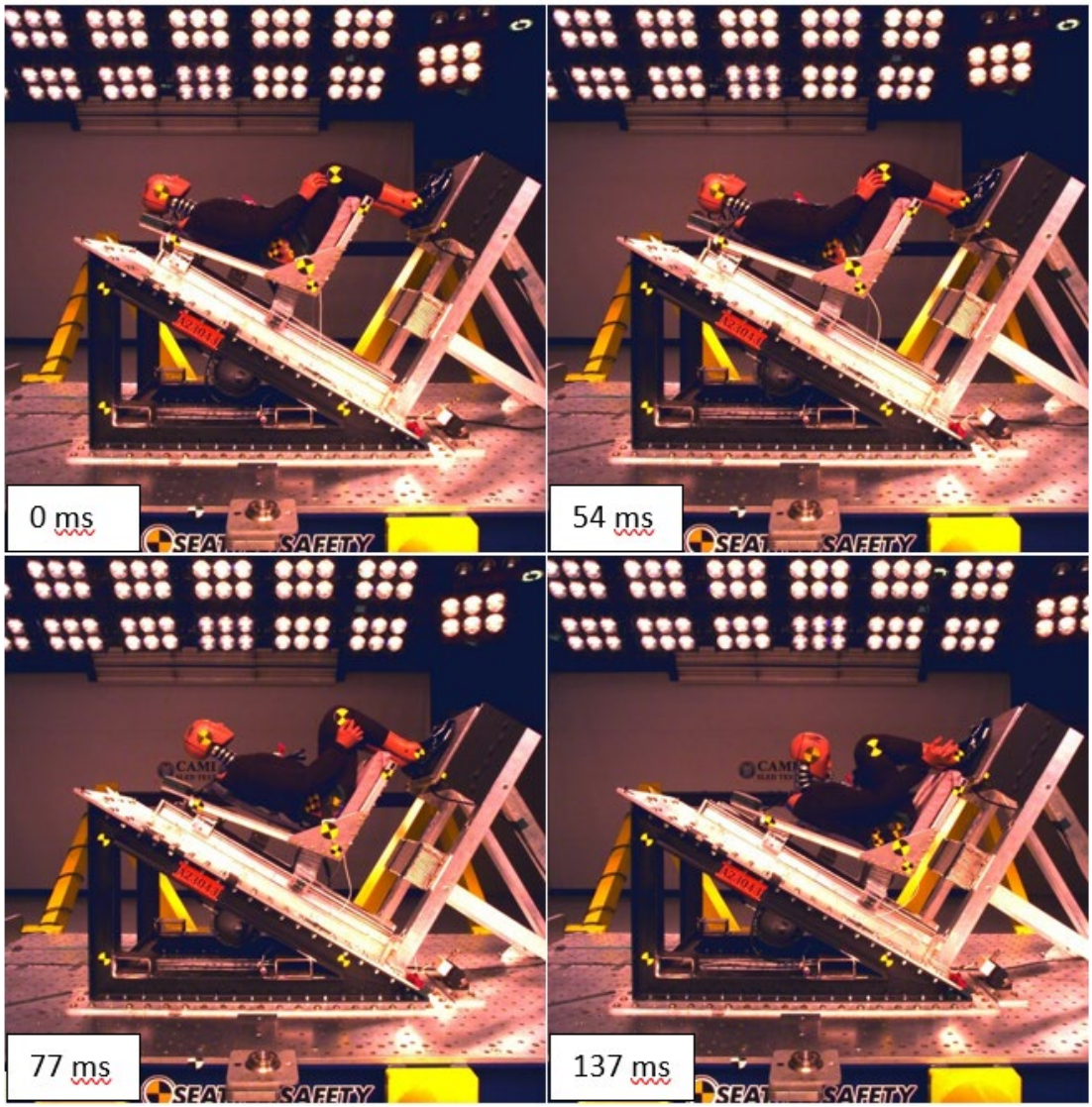

Figure 17: REAL Seat Exposed to the 30-g Pulse.

DISCUSSION

Comparison of Seat Stroke Distance at 1500 lb. Lumbar Load Limit

The ARAC report estimated the seat stroke necessary to not exceed the 1500 lb. lumbar load limit defined in §2X.562. Table 8 summarizes the minimum seat stroke distances calculated by CAMI and estimated by ARAC that are required to limit the lumbar load to 1500 lb. at the three tested sled pulses.

- 30 ft/sec pulse (30 g):
  - ARAC estimated a minimum seat stroke of 4.6 in.
  - This CAMI test series trendline (Equation 1) indicates 4.9 in., about 7% greater than ARAC.

- 25 ft/sec pulse (27.5 g):
  - ARAC estimated a minimum seat stroke of 2.8 in.
  - This CAMI test series trendline (Equation 2) indicates 3.4 in., about 21% greater than ARAC.
- 20.5 ft/sec pulse (25 g):
  - The ARAC did not provide estimates for this pulse.
  - This CAMI test series trendline (Equation 3) indicates a seat stroke of 1.4 in. would be necessary.

Table 8: Minimum Seat Stroke Needed to Limit Lumbar Load to 1500 lb.

Input Pulse (g)	CAMI Calculation (in.)	ARAC Estimate (in.)
25	1.4	N/A
27.5	3.4	2.8
30	4.9	4.6

Spinal Injury Risk

The Dynamic Response Index (DRI) is a model used to assess lumbar spine injury risk during vertical loading by representing the spinal column as a mass-spring-damper system (Stech, et. al., 1969). It uses seat pan accelerations as input and correlates the maximum DRI response to spinal injury data, primarily derived from military ejection studies. Since it was developed for rigid ejection seats with thin and firm cushions, the DRI could have limitations for application to typical aircraft seats due to the range of occupants and variety of cushions. Loads measured by the ATD were seen as a better means of determining the risk of injury. Consequently, the FAA developed a lumbar load tolerance value based on a correlation between lumbar load and DRI (DeWeese, et. al., 2021). A lumbar load of 1500 lb. correlates to a 9% spinal injury risk and serves as the FAA's pass/fail criterion for the lumbar spine. A 50% spinal injury risk corresponds to a 1710 lb. compression load, while a 1% risk aligns with a 1330 lb. load. Using Equation 1, Equation 2, and Equation 3, the seat stroke values for each sled pulse and injury risk level were calculated, as shown in *Table 9*, which indicates the seat stroke required to limit the lumbar load for each risk level.

Table 9: Spinal Injury Risk for Seat Stroke.

% of Spinal Injury Risk	Lumbar Load (lb.)	30.0 g – Seat Stroke (in.)	27.5 g – Seat Stroke (in.)	25.0 g – Seat Stoke (in.)	Pelvis Acceleration (g)
50	1710	3.8	2.5	1.0	23.5
9	1500	4.9	3.4	1.4	21.0
1	1330	6.1	4.3	2.0	19.0

Based on the relationship between pelvis acceleration and lumbar load (Equation 7*)* and the lumbar load values in Table 9 the occupant injury risk is quantified as follows: a 50% chance of spinal injury corresponds to a pelvis acceleration of 23.5 g; a 9% chance corresponds to 21.0 g; and a 1% chance corresponds to 19.0 g.

Lumbar Load versus Pelvis Acceleration Across Different Sled Pulses

To determine if the relation between lumbar load and pelvis acceleration shown in this report holds for sled pulses with lower peak accelerations, CAMI utilized 88 previous rigid seat tests that measured lumbar load and pelvis acceleration. The first set of data are 64 rigid seat tests with the §25.562 vertical sled pulse (14 g) and a Hybrid II ATD (DeWeese, 2006). These tests were conducted at CAMI between 2004 and 2005. The series tested a range of cushion variables, including thickness ranging from 1.0 in. to 4.5 in., open and closed cell foams, monolithic and cushion buildups, and multiple foam materials. In 2012, the Hybrid II, FAA-Hybrid III, and THOR ATDs were evaluated using three sled pulses: 9 g (200 ms duration), the 14 g §25.562 pulse, and the 19 g §23.562 pulse for pilot seats (Taylor, et. al., 2017b). All tests used a 1 in. thick Confor™ 47 cushion. Six tests included both a lumbar load cell and a pelvis accelerometer (three each with the Hybrid II and FAA-Hybrid III ATDs). Lastly, in 2015, 18 rigid seat tests with an FAA-Hybrid III ATD were tested at 14 g and 19 g with two densities of Confor™ foam (CF-42 and CF-45), two thicknesses (2 in. and 4 in.), and two formulations (original and "AC") (Taylor, et. al., 2017a). All 88 tests were run on the same rigid seat. The ideal sled pulses for the four test conditions from this report and the three test conditions from the historical data are shown in *Figure 18*.

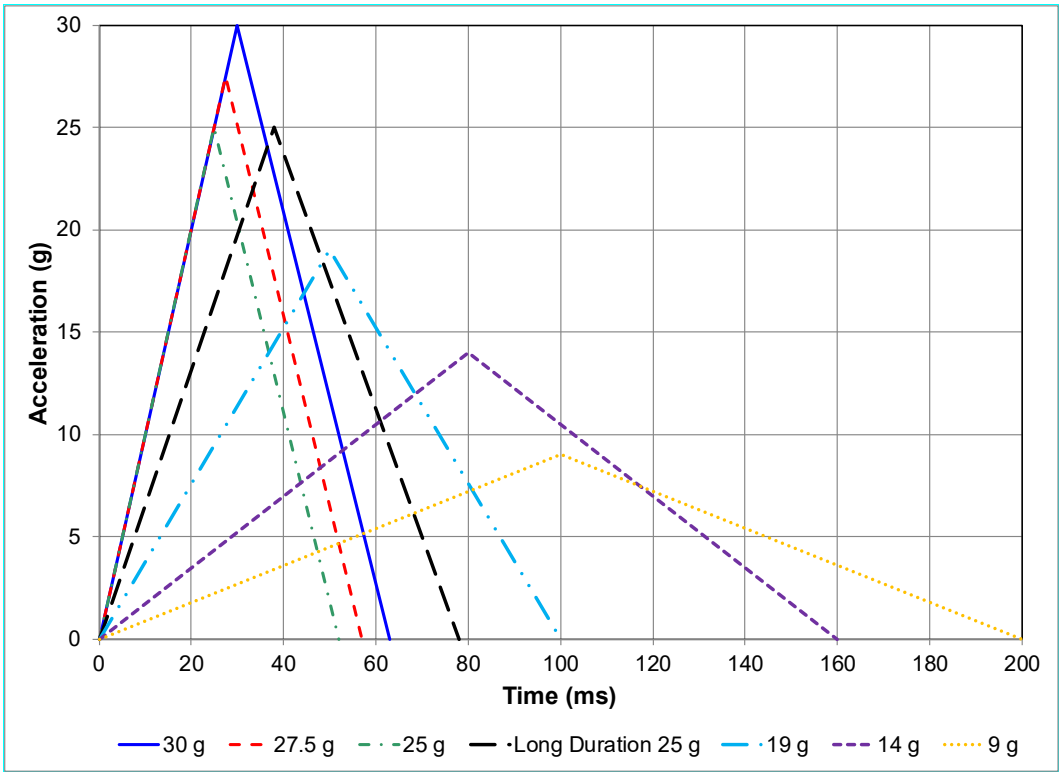

Figure 18: Ideal Sled Accelerations for Current and Historical Data Sets.

A linear trend line was fit to the 74 tests run with the §25.562 (14 g) sled pulse (*Figure 19*). The data has more scatter (R^2 = 0.8649) compared to the tests in the current project (R^2 = 0.9685), but the trend is still strong (Equation 15). Comparing Equation 7 with Equation 15, the slope of the current data is 2.6 times higher than the 14 g data (85 vs 33), indicating that the correlation between lumbar load and pelvis acceleration is dependent on the input conditions.

The equation for the linear trendline for the 2004 – 14-g data (R^2=0.8872) is:

$$Lumbar\ Load\ = 33.087 * Pelvis\ Acceleration + 520.87 \text{ (Equation 15)}$$

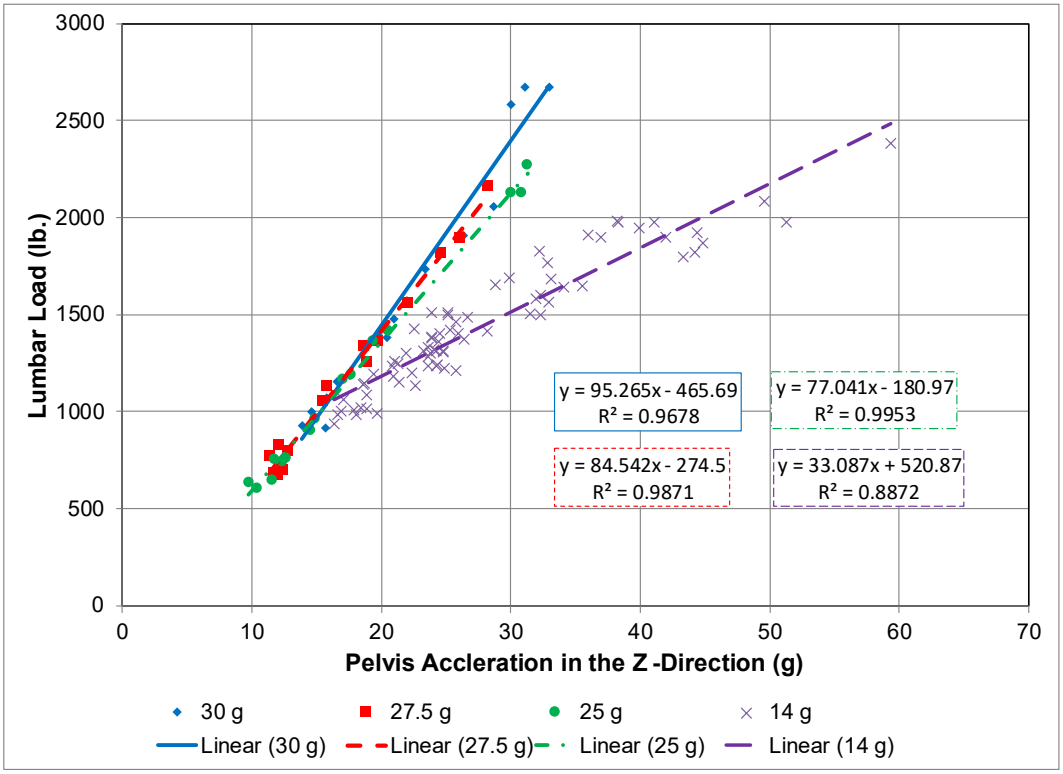

Figure 19: Pelvis Acceleration versus Lumbar Load for the Three Test Conditions Plus 14-g Data.

Figure 20 shows the trend lines for the current data (labeled 2023 data) and the 14-g data, along with individual points for the two 9-g tests from 2015, the ten 19-g tests from 2012 and 2015, and the three long duration 25-g tests from this series. The 9-g and long duration 25-g data fall on the 2023 curve, however the 19-g data falls between the 2023 curve and the 14-g curve. This pattern suggests that the correlation between pelvis acceleration and lumbar load is sensitive to the test conditions (e.g., peak sled acceleration, rigid seat versus stroking seat).

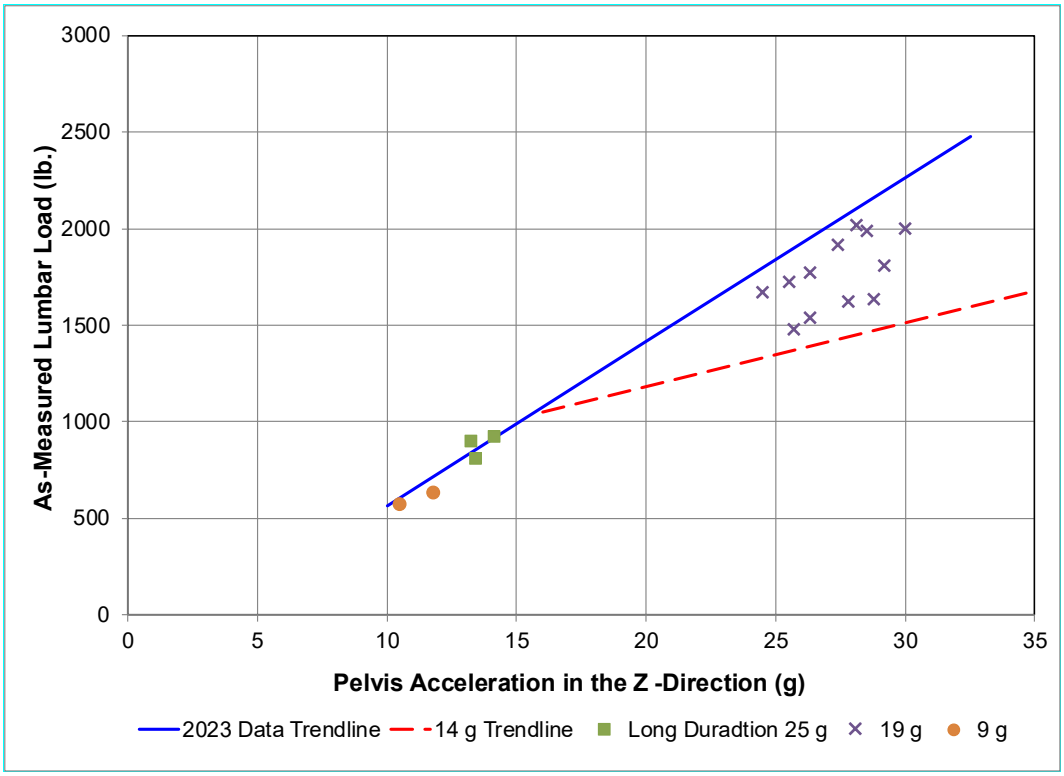

Figure 20: Lumbar Load versus Pelvis Acceleration for a Variety of Sled Acclerations.

Seat Pan Acceleration versus Seat Stroke

Coltman, et. al., calculated that 3.8 in. of seat stroke was needed to limit the seat pan acceleration to 12 g for a 50th percentile occupant (Coltman, et. al., 1985). The pulse referenced is an isosceles triangle characterized by a 25 g peak, a 65 ms duration, and a 26 ft/sec velocity change, configured for a purely vertical input. An equivalent pulse for an impact angle of 30° off vertical would have a 28.9 g peak and 30 ft/sec velocity change. This is most similar to the Part 27/29 pulse (30 g, 63 ms duration, and 30 ft/sec).

To limit the acceleration to 12 g, Equation 12 is rearranged to solve for the stroke distance, resulting in a required stroke of 15.2 inches for the 30 g trendline. This stroke length is four times the 3.8 inches reported by Coltman et al. The negative natural logarithmic trendline approaches an asymptote near 10 in. of seat stroke. Similarly, Equation 13 indicates that a seat stroke of 8.7 inches is necessary for the 27.5 g trendline, and Equation 14 shows that a seat stroke of 6.7 inches is required for the 25 g trendline. While this data suggests a substantially greater seat stroke requirement, even with the lowest peak-g test pulse, the discrepancy could be due to the discordant test configuration.

LIMITATIONS

Seat Cushion

This test series used a rigid seat pan, a 2-in. blue Confor™ 45 AC foam, and a 100% cotton cushion cover. Blue Confor is characterized by its high-rate sensitivity and stiffness which provides good coupling between the ATD and the seat pan (DeWeese, et. al., 2021). If a cushion with lower

rate sensitivity were used, it would likely result in greater dynamic overshoot of the ATD into the seat pan in the Z-direction, thereby increasing lumbar loads and the observed scatter. Previous testing suggests different cushions would change the correlations observed in this test series.

Occupant Response at Low Acceleration

This project was focused on loading conditions typically seen in certification. As a result, only one test had a pelvis acceleration below 10 g. Because the analysis has no data near the origin, the relationships derived may not generalize for pelvis accelerations below ~10 g. More detail is provided in Appendix A.

CONCLUSIONS

Emergency landing conditions of rotorcraft can result in severe loads being transmitted into the cabin. Therefore, the seating systems need to be designed to dissipate forces from being transferred to the occupant, commonly by means of seat deformation or compression. Many legacy rotorcraft lack sufficient space under the seat to meet the current Part 27 rules at the specified test condition (30 g deceleration input). The FAA's Biodynamics Research Team was tasked with mapping the risk of lumbar injury to sled pulse and seat stroke distance.

Forty-eight tests were conducted with three sled pulses and six different nominal seat stroke distances. Tests were run with a reusable energy absorbing seat with a thin firm cushion and an FAA-Hybrid III ATD. An additional 88 historical tests were analyzed to determine if the trends held for different test conditions.

The following observations were noted:

- Lumbar load closely tracked the seat stroke using a natural logarithmic regression for each sled pulse tested ($R^2 > 0.97$).
- Lumbar load was linearly correlated to the pelvis acceleration and was independent of the sled input pulse for this stroking seat and this range of sled pulses.
- Data from previous testing, conducted at lower peak decelerations, showed that the correlation between pelvis acceleration and lumbar load is sensitive to the test condition. The slope for the current data was 2.6 times the 14 g data. The 19 g data fell between the other two datasets.
- The amount of seat stroke necessary to meet the 1500 lb. lumbar load defined in 14 CFR Part 27.562 was 4.9 in. for the 30 ft/sec, 30 g pulse defined in the regulation. The necessary seat stroke for the reduced velocity pulse proposed by the Aviation Rulemaking Advisory Committee (ARAC) was 3.4 in. These values differ from what the ARAC estimated, 4.6 in. and 2.8 in. respectively (*Table 8)*.

These findings may support updates to advisory circulars and guide future rulemaking for the retrofit of dynamic seats into existing type designs with the ultimate goal to enhance rotorcraft crashworthiness and increase occupant protection during accidents.

REFERENCES

Coltman, J. W., Bolukbasi, A. O., & Laananen, D. H. (1985). *Analysis of rotorcraft crash dynamics for development of improved crashworthiness design criteria* (DOT/FAA/CT-85/11). https://apps.dtic.mil/sti/tr/pdf/ADA158777.pdf

DeWeese, R. (2006). *Measurement of aircraft seat cushion dynamic properties and associated occupant lumbar spine loads using full-scale sled tests*. SAE General Aviation Technology Conference.

DeWeese, R., Moorcroft, D., & Taylor, A. (2021). *Lumbar load variability in dynamic testing of transport category aircraft seat cushions* (Office of Aerospace Medicine Report, DOT/FAA/AM21-09). Federal Aviation Administration. https://www.faa.gov/sites/faa.gov/files/data_research/research/med_humanfacs/oamtechreports/202109.pdf

Department of Defense (1999). Joint Service Specification Guide: Aircraft Crash Survival Design Criteria, JSSG-2010-7.

Federal Register. (2015). Department of Transportation, Federal Aviation Administration, Aviation Rulemaking Advisory Committee—New Task, Vol. 80, No. 214. https://www.federalregister.gov/documents/2015/11/05/2015-28151/aviation-rulemaking-advisory-committee-new-task

Gowdy, V., DeWeese, R., Beebe, M., Wade, B., Duncan, J., Kelly, R., & Blaker, J. (1999). *A lumbar spine modification to the Hybrid III ATD for aircraft seat tests*. SAE Technical Paper 1999-01-1609. https://doi.org/10.4271/1999-01-1609

Moorcroft, D., DeWeese, R., & Taylor, A. (2010). *Improving test repeatability and methods*. The Sixth Triennial International Fire & Cabin Safety Research Conference, October 25-28, 2010. https://www.fire.tc.faa.gov/2010Conference/files/Crash_Dynamics_III/MoorcroftLumbarLoad/MoorcroftLumbarLoadPres.pdf

Obermiller, D. (2023). *The why, how, and cautions of regression without an intercept*. SAS Communities. https://communities.sas.com/t5/SAS-Communities-Library/The-Why-How-and-Cautions-of-Regression-Without-an-Intercept/ta-p/894641

Rotorcraft Occupant Protection Working Group (ROPWG). (2016). *Tasks 1 and 2: Cost-benefit analysis report to the Aviation Rulemaking Advisory Committee (ARAC)*. https://www.faa.gov/regulations_policies/rulemaking/committees/documents/media/ROPWG%20Tasks%201%20and%202%20Report.pdf

Rotorcraft Occupant Protection Working Group (ROPWG). (2018). *Task 5 – Crash resistance fuel systems (CRFS) final analysis report to the Aviation Rulemaking Advisory Committee (ARAC)*. https://www.faa.gov/regulations_policies/rulemaking/committees/documents/index.cfm/document/information/documentID/3503/

Roskop, L. (2017). *Post-crash fire and blunt force fatal injuries in U.S. registered, type certificated rotorcraft*. 88th Annual Scientific Meeting, April 2017.

SAE International. (2022a). *Instrumentation for impact test part 1 - Electronic instrumentation* (SAE Standard J211/1_202208). https://doi.org/10.4271/J211/1_202208

SAE International. (2022b). *Instrumentation for impact test part 2 - Electronic instrumentation* (SAE Standard J211/2_202208). https://doi.org/10.4271/J211/2_202208

SAE International. (2024). *Sign convention for vehicle crash testing* (SAE Standard J1733_202411). https://doi.org/10.4271/J1733_202411

SAE International. (2020). *Performance standard for seats in civil rotorcraft, transport aircraft, and general aviation aircraft* (SAE Standard AS8049D). https://doi.org/10.4271/AS8049D

Stech, E., & Payne, P. (1969). *Dynamic models of the human body* (AMRL-TR-66-15). Aerospace Medical Research Laboratory, Wright-Patterson AFB, Ohio.

Taylor, A., DeWeese, R., & Moorcroft, D. (2017a). *Comparison of AC and original formulation Confor foam performance in civil aircraft vertical impact tests* (Report No. DOT/FAA/AM-17/1). Civil Aerospace Medical Institute; United States Office of Aerospace Medicine. https://rosap.ntl.bts.gov/view/dot/35555

Taylor, A., Moorcroft, D., & DeWeese, R. (2017b). *Comparison of the Hybrid II, FAA Hybrid III, and THOR-NT in vertical impacts*. AHS International 73rd Annual Forum & Technology Display, Fort Worth, Texas, USA, May 9–11, 2017.

Taylor, A., Pellettiere, J. (2022) Fatal Rotorcraft Accidents in Ten-Year Period. Vertical Flight Society. https://doi.org/10.4050/F-0078-2022-17500

U.S. Code of Federal Regulations. (2024). Title 14 Part 27.562. Washington, DC: U.S. Government Printing Office. https://www.govinfo.gov/app/details/CFR-2024-title14-vol1/CFR-2024-title14-vol1-sec27-562

U.S. Code of Federal Regulations. (2024). Title 14 Part 29.562. Washington, DC: U.S. Government Printing Office. https://www.govinfo.gov/app/details/CFR-2024-title14-vol1/CFR-2024-title14-vol1-sec29-562

APPENDIX A

The data in this report was initially analyzed using trendlines that were forced through the origin (*Figure 21*). This is referred to as regression without an intercept and results in a model with the form y = mx. In this example, which compares the measured lumbar load to the pelvis acceleration, the assumption is that if the accelerometer reads zero, then the load cell must read zero as well[3]. This yields an equation where the lumbar load is equal to 71.662 times the pelvis acceleration, which is reasonable considering the mass of the ATD above the load cell is approximately 75 lb.[4]. To evaluate the correlation of these two channels, a goodness-of-fit measure (R-squared) is used. Using the linear regression without an intercept, the R-squared value for this data is 0.99. This is suspect considering that the "best" fit, which is not forced through the origin (lumbar load equals 84.938 times pelvis acceleration – 283.78 lb.), produces an R-squared of 0.97. From statistics literature, the interpretation of R-Square for regressions without an intercept "is no longer the proportion of variance explained and does not have a clear interpretation" (Obermiller, 2023).

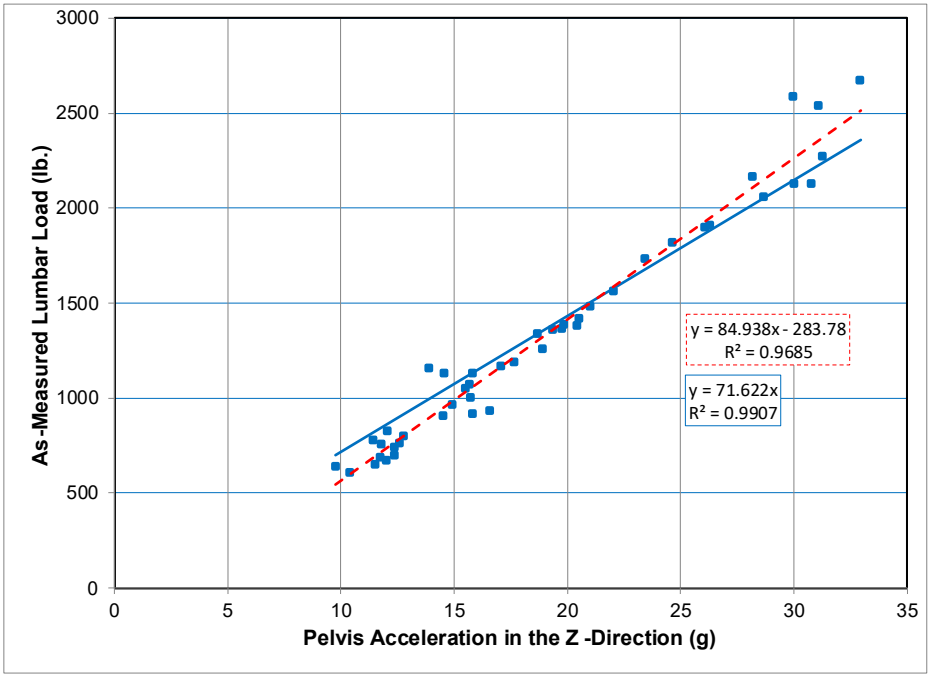

Figure 21: Intercept vs Non-Intercept Trendlines for Same Data Set.

[3] The standard test setup involves zeroing load cells and accelerometers right before the sled pulse begins. While there is load acting on the load cell from the upper half of the ATD when there is no motion, this load is removed from the measurement by convention.

[4] In this scenario, the linear regression without intercept (y=mx) is equal to Newton's second law: force equals mass times acceleration, written as F=ma.

The calculated intercept of the linear regression line results in a lumbar load of 283.78 lb. at an acceleration of zero. This does not align with the assumed physics of zero measured force at zero acceleration. The previously referenced statistics discussion notes three potential explanations.

1. The data is not best explained by a linear model.
    a. This explanation was evaluated by selecting alternative trendlines in Excel. An exponential fit produced no solution, and a polynomial fit produced an R-squared of 0.9763. The polynomial was a better fit than the linear only in the 2nd decimal place.
2. When there is no data close to the origin, "we probably should not assume the linear relationship seen with this data holds all the way to the origin (Obermiller, 2023)."
    a. Our data set does not contain pelvis accelerations below 10 g. While there is a physical rationale for assuming zero load at zero acceleration, data to show the trend between 0 an 10 g is unavailable.
3. The non-zero intercept could be within the bounds of error on the measurements.
    a. This explanation seems most probable, although the 283 lb. is slightly higher than is expected for lumbar load variance of 150-200 lb. (DeWeese, et. al. 2021).

The goal of this evaluation was to determine whether pelvis acceleration could be used instead of lumbar load. Thus, it is more important to look at values around the pass/fail criteria than values at zero. The two curves intersect at a pelvis acceleration of 21.5 g and lumbar load of 1546 lb. Because of this, a pelvis acceleration pass/fail criterion would be nearly the same regardless of which regression model is chosen: 20.9 g without intercept (i.e. y=mx) and 21.0 g with intercept (i.e. y = mx+b). *Table 10* shows the lumbar load from the two regression models within a corridor of 10 g to 24 g of pelvis acceleration. Because the R^2 value for the regression with an intercept provides the goodness of fit, this report uses this method instead of forcing the equation through zero.

Table 10: Lumbar Load Calculated with and without an Intercept.

Pelvis Accel (g)	Lumbar Load (Linear w/ Int) (lb.)	Lumbar Load (Linear w/o Int) (lb.)
10.0	566	718
12.0	735	861
14.0	905	1005
16.0	1075	1148
20.0	1415	1435
21.0	1500	1504
24.0	1755	1719

APPENDIX B

Dataset and Contact Information

Title: Occupant Response to Varying Seat Stroke Using a Reusable Energy Attenuating Aircraft Seat

Principal Investigator: Ian Hellstrom – ORCID: 0000-0002-3972-3981

Affiliation: U.S. Department of Transportation, Federal Aviation Administration, Civil Aerospace Medical Institute

Contact Information: Aerospace Medical Research Division, 6500 S. MacArthur Blvd, AAM-632, Oklahoma City, OK 73169, Ian.T.Hellstrom@faa.gov, 405-954-5767

https://www.faa.gov/about/office_org/headquarters_offices/avs/offices/aam/cami/

Funder: Federal Aviation Administration (faa.gov)

Grant/Contract(s): N/A

Persistent link: https://doi.org/10.21949/1529692

Recommended Citation: Hellstrom, I., Moorcroft, D., Carroll, W. (2025). Occupant Response to Varying Seat Stroke Using a Reusable Energy Attenuating Aircraft Seat [datasets]. U.S. Department of Transportation, Federal Aviation Administration. https://doi.org/10.21949/1529692

Project Abstract

While the U.S. rotorcraft accident rate over the past 10 years has steadily decreased, the number of fatal rotorcraft accidents and fatalities remains virtually unchanged. Survival in many impact scenarios is directly related to the certification level of the rotorcraft. Seats installed in newly designed rotorcraft must meet the emergency landing dynamic conditions rule (14 CFR Part 27.562 and §29.562). Rotorcraft with existing type certificates, whether newly manufactured or not, do not need to meet the dynamic rule. Many legacy rotorcraft have limited space beneath the existing seats, this precludes the use of a retrofitted fully compliant stroking seat. However, these rotorcraft could still benefit from meeting the framework of the rule with a reduced velocity requirement. The FAA Civil Aerospace Medical Institute conducted research on the relationship between impact pulse, seat stroke, and occupant injury risk. 48 tests were run using a rigid Reusable Energy Attenuating Laboratory (REAL) Seat, designed by the Navy, that allowed for varying seat stroke between tests. Results showed a strong correlation between seat stroke distance and lumbar load (R^2>0.97), as well as pelvis acceleration and lumbar load. Comparing the data from this test series to 88 tests from the CAMI database showed that the relationship between pelvic acceleration and lumbar load is dependent on the sled acceleration. These findings may support updates to advisory circulars and guide future rulemaking to enhance rotorcraft crashworthiness.

Project start date: 10-08-2020

Project end date: 9-30-2025

Data Description

This dataset contains sled test data of anthropomorphic test devices seated in an energy attenuating seat system. This data is created by physical experiments. Sensors include load cells and accelerometers. Data also includes video from high-speed cameras and photos from still cameras. The tests were conducted in 2023. No existing data were used for this test series.

It is anticipated that aircraft seat manufacturers and test laboratories will benefit from access to this data as they design and test real aircraft seats and restraints. This dataset will also provide a public record to support potential rulemaking.

Roles & Responsibilities

The FAA Aerospace Medical Research Division (see Contact Information) is responsible for generating the data and is responsible for managing the data initially. This division is responsible for managing the internal project management processes to ensure adherence to the published data management plan (DMP). This process requires management review and sign-off at project start and close-out.

This dataset is hosted by NHSTA in the biodynamics test database at:

https://www.nhtsa.gov/research-data/research-testing-databases#/biomechanics

Standards Used

The dataset complies with the NHTSA Test Reference Guide available at https://www.nhtsa.gov/databases-and-software/entree-windows. The data files collected are saved in common file formats, including ascii text, .xls, .jpg, .avi, and .mp4. The file formats can be opened using commonly available software such as text editors, picture viewers, and video viewers. .xls files can be opened with Microsoft Excel or freely available software, such as OpenRefine.

Access Policies

These data files are in the public domain and can be shared without restriction. The data files contain no sensitive information.

Sensitive Data Policies

The data files contain no sensitive information.

Sharing Policies

The data are in the public domain and may be re-used without restriction. Citation of the data is appreciated. Please use the following recommended citation: Hellstrom, I., Moorcroft, D., Carroll, W. (2024). Occupant Response to Varying Seat Stroke Using a Reusable Energy Attenuating Aircraft Seat [datasets]. U.S. Department of Transportation, Federal Aviation Administration. https://doi.org/10.21949/1529693

Archiving and Preservation Plans

Crash Test Database (which includes Vehicle, Biomechanics, and Component databases) is stored in the Amazon Aurora PostgreSQL database. The database is hosted in the DOT managed

Amazon Web Services (AWS) cloud environment. Automated full database backups are taken daily, leveraging AWS relational database service backups. The retention period for the backups is 14 days. The database is secure and only accessible to selected DOT users while only on the DOT network.

The dataset will be retained in perpetuity.

FAA staff will mint persistent Digital Object Identifiers (DOIs) for each dataset stored in the Biomechanics Test Database. These DOIs will be associated with dataset documentation as soon as they become available for use. The Digital Object Identifiers (DOIs) associated with this dataset include: https://doi.org/10.21949/1529693.

The assigned DOI resolves to the repository landing page for the “Occupant Response to Varying Seat Stroke Using a Reusable Energy Attenuating Aircraft Seat” dataset, so that users may locate associated metadata and supporting files.

The Biomechanics Test Database meets all the criteria outlined on the “Guidelines for Evaluating Repositories for Conformance with the DOT Public Access Plan” page: https://ntl.bts.gov/ntl/public-access/guidelines-evaluating-repositories.

Applicable Laws and Policies

This data management plan was created to meet the requirements enumerated in the U.S. Department of Transportation's 'Plan to Increase Public Access to the Results of Federally-Funded Scientific Research' Version 1.1 https://doi.org/10.21949/1529692 and guidelines suggested by the DOT Public Access website https://doi.org/10.21949/1529693, in effect and current as of April 29, 2024.